

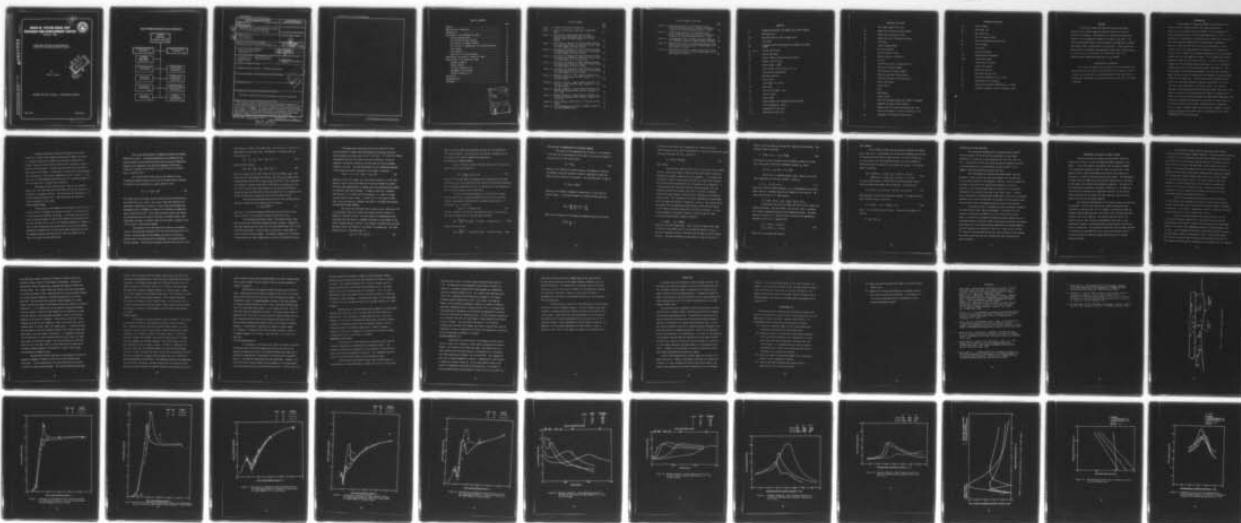
AD-A037 062

DAVID W TAYLOR NAVAL SHIP RESEARCH AND DEVELOPMENT CE--ETC F/6 1/3
A NONLINEAR VERTICAL-PLANE MATHEMATICAL MODEL FOR AIR CUSHION-S--ETC(U)
JUN 76 D D MORAN
SPD-615-05

UNCLASSIFIED

NL

1 OF 1
AD
A0 37062



END

DATE
FILMED
4-77

SPD-615-05

AD A 037062

A NONLINEAR VERTICAL-PLANE MATHEMATICAL MODEL
FOR AIR CUSHION-SUPPORTED VEHICLES

**DAVID W. TAYLOR NAVAL SHIP
RESEARCH AND DEVELOPMENT CENTER**

Bethesda, Md. 20084

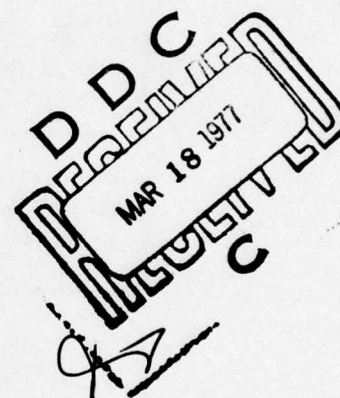


12
B.51

A NONLINEAR VERTICAL-PLANE MATHEMATICAL
MODEL FOR AIR CUSHION SUPPORTED VEHICLES

by

David D. Moran



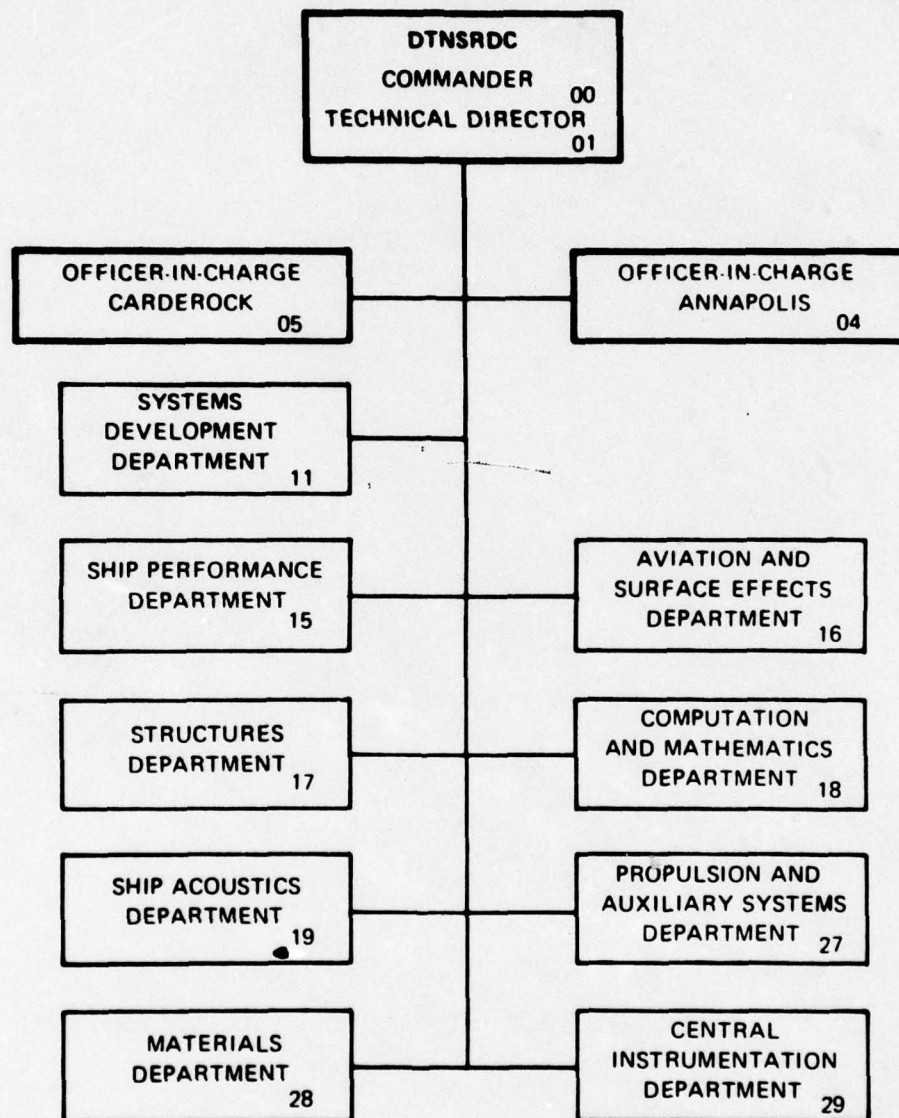
APPROVED FOR PUBLIC RELEASE: DISTRIBUTION UNLIMITED

JUNE 1976

SPD-615-05

ENCLOSURE (1)

MAJOR DTNSRDC ORGANIZATIONAL COMPONENTS



UNCLASSIFIED

SECURITY CLASSIFICATION OF THIS PAGE (When Data Entered)

REPORT DOCUMENTATION PAGE		READ INSTRUCTIONS BEFORE COMPLETING FORM
1. REPORT NUMBER (14) SPD-615-05 ✓	2. GOVT ACCESSION NO.	3. RECIPIENT'S CATALOG NUMBER
4. TITLE (and Subtitle) (6) A Nonlinear Vertical-Plane Mathematical Model for Air Cushion-Supported Vehicles		5. TYPE OF REPORT & PERIOD COVERED
7. AUTHOR(s) (10) David D./Moran		6. PERFORMING ORG. REPORT NUMBER
9. PERFORMING ORGANIZATION NAME AND ADDRESS David W. Taylor Naval Ship Research and Development Center, Ship Performance Department ✓		8. CONTRACT OR GRANT NUMBER(s) (17) PAAR
11. CONTROLLING OFFICE NAME AND ADDRESS Naval Sea Systems Command Washington, D.C.		10. PROGRAM ELEMENT, PROJECT, TASK AREA & WORK UNIT NUMBERS Task Area S1417 Task 14174 Work Unit Number 1-1180-004
14. MONITORING AGENCY NAME & ADDRESS (if different from Controlling Office) (12) 56p. (16) S1417		12. REPORT DATE (11) June 1976
		13. NUMBER OF PAGES 56
		15. SECURITY CLASS. (of this report) UNCLASSIFIED
16. DISTRIBUTION STATEMENT (of this Report) APPROVED FOR PUBLIC RELEASE: DISTRIBUTION UNLIMITED		15a. DECLASSIFICATION/DOWNGRADING SCHEDULE
17. DISTRIBUTION STATEMENT (of the abstract entered in Block 20, if different from Report)		
18. SUPPLEMENTARY NOTES		
19. KEY WORDS (Continue on reverse side if necessary and identify by block number) ACV Motion Simulation; ACV Overland Response; Pressure Distribution		
20. ABSTRACT (Continue on reverse side if necessary and identify by block number) An analytical model for predicting the pitch and heave response of air-cushion-supported vehicles (ACV) during overland operation is developed. The effects of air compressibility and skirt contact with the supporting surface are included in the model. The resulting analytical model is used to predict the response of a JEFF (B) experimental model to periodically varying terrain. These predictions show excellent correlation with experimental model data, thereby serving as verification of the accuracy of the analytical model for a complete range of operating conditions for the JEFF (B).		

DD FORM 1473
1 JAN 73EDITION OF 1 NOV 65 IS OBSOLETE
S/N 0102-014-6601

UNCLASSIFIED

SECURITY CLASSIFICATION OF THIS PAGE (When Data Entered)

389 694

SECURITY CLASSIFICATION OF THIS PAGE(When Data Entered)

TABLE OF CONTENTS

	Page
ABSTRACT	1
ADMINISTRATIVE INFORMATION	1
INTRODUCTION	2
DEVELOPMENT OF THE MATHEMATICAL MODEL	3
CUSHION PRESSURE MODEL	5
AIR FLOW DUE TO CRAFT PUMPING	8
AIR FLOW DUE TO TERRAIN PUMPING	9
AIR FLOW DUE TO COMPRESSIBILITY OR CUSHION PUMPING	10
SKIRT FORCES	11
SKIRT MOMENTS	13
SOLUTION OF AIR FLOW EQUATIONS	14
EXPERIMENTAL VALIDATION OF ANALYTICAL MODEL	15
APPLICATIONS OF THE ANALYTICAL MODEL	18
RESPONSE LINEARITY	18
TERRAIN PUMPING	20
LIFT FAN CHARACTERISTICS	21
SUBHARMONIC OSCILLATIONS	22
CUSHION COMPRESSIBILITY	23
CONCLUSIONS	25
RECOMMENDATIONS	26
REFERENCES	28

ACCESSION FOR		
RTIS	Write Section	<input checked="" type="checkbox"/>
DPC	Build Section	<input type="checkbox"/>
UNANNOUNCED		
JUSTIFICATION		
BY		
DISTRIBUTION/AVAILABILITY CODES		
Dist.	AVAIL. and/or SPECIAL	

LIST OF FIGURES

	Page
Figure 1 - JEFF(B) Lift System Configuration	30
Figure 2 - Bow Skirt Configuration Employed in Analytical Model	31
Figure 3 - Correlation of Theoretical Pitch Transfer Function with Experimental Data as a Function of Wave Length for Model Speeds of 4, 6, and 8 Knots	32
Figure 4 - Correlation of Theoretical Pitch Transfer Function with Experimental Data as a Function of Wave Length for Model Speeds of 10 and 12 Knots	33
Figure 5 - Correlation of Theoretical Pitch Transfer Function with Experimental Data as a Function of Wave Length for Model Speeds of 13 and 15 Knots	34
Figure 6 - Correlation of Theoretical Heave Transfer Function with Experimental Data as a Function of Wave Length for Model Speeds of 4, 6, and 8 Knots	35
Figure 7 - Correlation of Theoretical Heave Transfer Function with Experimental Data as a Function of Wave Length for Model Speeds of 10 and 12 Knots	36
Figure 8 - Correlation of Theoretical Heave Transfer Function with Experimental Data as a Function of Wave Length for Model Speeds of 13 and 15 Knots	37
Figure 9 - Response Linearity: Pitch Transfer Function as a Function of Wave Slope for Model Speeds of 11, 13.5, 16, and 18 Knots	38
Figure 10 - Response Linearity: Heave Transfer Function as a Function of Wave Slope for Model Speeds of 11, 13.5, 16, and 18 Knots	39
Figure 11 - Response Linearity: Pitch Transfer Function as a Function of Nondimensional Encounter Frequency for $\lambda/L = 1.65$	40
Figure 12 - Response Linearity: Heave Transfer Function as a Function of Nondimensional Encounter Frequency for $\lambda/L = 1.65$	41
Figure 13 - Terrain Pumping Coefficients as a Function of Wave Length	42
Figure 14 - Fan Performance Curves Used in Parametric Study of Lift Fan Characteristics	43

LIST OF FIGURES (continued)

	Page
Figure 15 - Parametric Study of Lift Fan Characteristics: Pitch Transfer Function as a Function of Encounter Frequency for Various Fan Maps with $\lambda/L = 1.65$	44
Figure 16 - Parametric Study of Lift Fan Characteristics: Heave Transfer Function as a Function of Encounter Frequency for Various Fan Maps with $\lambda/L = 1.65$	45
Figure 17 - Time-Dependent Pitch and Heave Simulation Responses for Sinusoidal Terrain at a Model Speed of 18 Knots	46
Figure 18 - Compressibility Effect on Model Scale Analytic Pitch Transfer Function as a Function of Wave Length for a Model Speed of 15 Knots	47
Figure 19 - Compressibility Effect on Model Scale Analytic Heave Transfer Function as a Function of Wave Length for a Model Speed of 15 Knots	48

NOTATION

A_i	Leakage area between fan chamber and cushion chamber
a	Wave amplitude
a/L	Wave amplitude to cushion length ratio
B	Craft beam
C_{Di}	Discharge coefficient between fan chamber and cushion chamber
C_1, C_2, C_3	Fan map coefficients
d_2	Cushion bag chord
d_3	Cushion chamber extension due to contact
F	Contact vertical force
F_n	Froude number, U/\sqrt{Lg}
F_v	Total contact vertical force, $F_1 + F_2$
g	Gravitational acceleration
H	Heaviside function
h_k	Skirt height
I	Craft moment of inertia
ka	Wave slope
k_w	Terrain wave number, $2\pi/\lambda$
L	Cushion length
L_s	Skirt height
l	Height between skirt edge and terrain surface
l'	Skirt submergence, $-lH(-l)$
l'_a	Deformation of aft skirt
l'_b	Deformation of bow skirt

NOTATION (continued)

M	Total moment about the y axis
M_C	Moment due to vertical contact forces
M_F	Moment due to contact friction
M_R	Moment due to air flow reaction forces
m	Craft mass
P	Cushion guage pressure
P_f	Fan gauge pressure
p	Cushion pressure, total
p_a	Ambient pressure, atmospheric
Q	Air flow
Q_c	Effective flow due to compressibility
Q_e	Flow out of cushion chamber
Q_i	Flow from fan to cushion chamber
Q_m	Effective flow due to craft motion
Q_w	Effective flow due to terrain pumping
R_c	Cushion bag radius
S	Cushion area
t	Time
U	Model speed
V	Cushion volume
x	Positive coordinate along craft length (+ forward)
x_g	Component of center of mass along x
\bar{x}	Moment arm of the cushion area along the y axis
z	Positive coordinate in vertical direction (+ up)
z_g	Component of the center of mass along z

NOTATION (continued)

z_w	Terrain height
α_a	Seal angle, aft
α_b	Seal angle, bow
γ	Ratio of specific heats
ΔP	Pressure difference across orifice
Δt	Time increment
θ	Pitch angle
λ	Terrain wavelength
λ/L	Nondimensional wavelength
$\lambda/2a$	Inverse wave slope
μ	Coefficient of friction
ρ	Cushion gas density
ρ_a	Ambient gas density
ϕ	Nondimensional fan flow
ϕ_o	Design flow coefficient, $\phi_o = 0.142$
ψ	Nondimensional fan pressure
ψ_o	Design point pressure coefficient, $\psi_o = 0.054$
ω	Encounter frequency, terrain frequency, $2\pi U/\lambda$

ABSTRACT

An analytical model for predicting the pitch and heave response of air-cushion-supported vehicles (ACV) during overland operation is developed. The effects of air compressibility and skirt contact with the supporting surface are included in the model. The resulting analytical model is used to predict the response of a JEFF(B) experimental model to periodically varying terrain. These predictions show excellent correlation with experimental model data, thereby serving as verification of the accuracy of the analytical model for a complete range of operating conditions for the JEFF(B).

ADMINISTRATIVE INFORMATION

This study was sponsored by the Naval Sea Systems Command under Task Area S1417, Task 14174; and administered by the Amphibious Assault Landing Craft Program Office, Systems Development Department, David W. Taylor Naval Ship Research and Development Center under Work Unit Number 1-1180-004.

INTRODUCTION

The development of analytical models for the prediction of the motion of air cushion vehicles over random surfaces has proved to be an extremely difficult problem. Only a few analytical models have shown promise of success (See References 1,2,3,8,9)*. The difficulties in developing a suitable analytical model are attributed to the strong nonlinear characteristics of the physical phenomena in question. These nonlinearities arise from the deformation of the vehicle skirts, the complicated air flow patterns in the supporting cushions, and in general the nonlinear characteristics of the interface between the craft and supporting surface. If the supporting surface is deformable, additional nonlinearities arise. In order to eventually produce craft having optimum design characteristics, it is necessary to develop analytical tools that accurately model craft behavior. This report presents the successful development of a nonlinear time-domain model that can be used for predicting craft response in pitch and heave during overland operations. The analytical model developed does not contain any artificial damping or restoring coefficients, artificial inertial or mass properties, or artificial tuning. All parameters employed are derived directly from the physical system under study. The degree of success of the current analytical model is indicated by the excellent correlation results achieved with experimental model data. The simulations conducted for purposes of verification included prediction of pitch and heave for motion over sinusoidal terrain, trapezoidal terrain, ramps, triangular bumps, and step function changes in terrain. The more interesting sinusoidal results are presented in this report.

*References are listed on page 28.

The analytical model presented in this report is appropriate for a model scale craft. Once the analytical model is fully developed, generalization to full scale requires only a straightforward process of changing geometrical parameters to full scale values. The full scale analytical model can be used in an extremely cost effective manner for design optimization studies, trade-off studies, and performance predictions.

DEVELOPMENT OF THE MATHEMATICAL MODEL

The air cushion vehicle configuration considered in the analytic model consists of a fully-skirted perimeter with two supporting air cushions separated by a transverse stability skirt. The air cushions and peripheral skirts are supplied with air from a fan chamber, which in turn is supplied with air from the lift fan. This general configuration, which is illustrated in Figure 1, is representative of the Amphibious Assault Landing Craft (AALC) Program JEFF(B) craft.

All mathematical models are developed in a body centered coordinate system having the z axis directed upward and the x axis forward. Positive pitch corresponds to a bow up orientation. The analytic model has been developed to compute ACV motion in three degrees of freedom, specifically pitch, heave, and surge. Only pitch and heave results are presented in this report since experimental data including surge was not available for validation purposes. Means have been developed to extend the present mathematical model to include all six degrees of freedom.

The basic equation of motion for heave is given by

$$m\ddot{z} = P_1 S_1 + P_2 S_2 + F_v - mg \quad (1)$$

where* the products $P_1 S_1$ and $P_2 S_2$ represent the vertical force arising from the forward and aft cushions, F_v represents the vertical force arising from skirt contact with the supporting surface, and mg represents the gravitational force. The differential equation describing pitch is given by

$$\begin{aligned} I\ddot{\theta} = & P_1 S_1 (\bar{x}_1 - x_g) + P_2 S_2 (\bar{x}_2 - x_g) + M \\ & + P_1 B(h_{k1} - h_{k3}) \{z_g + \frac{1}{2} (h_{k1} + h_{k3})\} \\ & + P_2 B(h_{k3} - h_{k2}) \{z_g + \frac{1}{2} (h_{k3} + h_{k2})\} \end{aligned} \quad (2)$$

The first two expressions appearing on the right hand side of the above equation represent the pitching moment arising from the forward and aft cushion pressure forces respectively. M represents the moment produced by skirt contact with the supporting surface and arising from air escaping under the skirts. The last two terms represent moments identified with the pressure differentials that exist across the skirts.

* A complete description of all symbols appears in the notation section.

The above second order differential equations are solved directly by a Taylor series expansion using evenly spaced time steps, Δt . Extensive sensitivity studies were conducted to determine an optimum integration time step and to assure that integration instabilities were not encountered. Various exciting forces were used during these sensitivity studies. In each case, the step size Δt was decreased until variations in final results remained less than 1 percent. A time step size of 0.0025 seconds proved sufficient for 1 percent accuracy for all cases examined in a model scale simulation.

Expressions for the various forces, moments, and pressures appearing on the right hand side of the above differential equations are developed in subsequent sections. The expressions are implemented in a digital computer program which is used to generate the predicted results presented in this report.

CUSHION PRESSURE MODEL

The pressure in each chamber of the segmented cushion of the air cushion vehicle is assumed to be spatially uniform, with forces acting at fixed centers of pressure, \bar{x}_1 and \bar{x}_2 . In the actual ACV there will exist a pressure gradient in each of the cushions arising mainly from the mass transfer of air (4, 5, 6). This pressure gradient will depend in part on craft orientation and velocities and in part on the changing geometrical characteristics of the solid surface supporting the craft. The changing pressure distribution will alter the location of the center of pressure during craft motion.

The current approximation is adequate provided the pressure gradients are small. A detailed examination of the effects of the pressure gradient would require solving a set of partial differential equations with temporally- and spatially-dependent coefficients. A numerical procedure of this type is currently being investigated under a separate effort.

For a given fan air flow rate, Q , the pressure in the intermediate chamber between the fan and the forward and aft cushions is assumed to be represented by a simple quadratic form,

$$P_f = C_1 + C_2 Q + C_3 Q^2 \quad (3)$$

This model takes into account ducting effects and fan characteristics. The coefficients C_1 - C_3 used in the current study were obtained from experiments conducted by the David W. Taylor Naval Ship Research and Development Center (DTNSRDC) on a model of the JEFF(B), an Amphibious Assault Landing Craft (6). This simple nonlinear equation was chosen for convenience and can be easily replaced by tabulated values, more complicated fan maps, or analytic models of the dynamic response of the lift fan and air distribution systems.

The pressures in the forward and aft cushions are obtained from air flow continuity equations and from discharge equations for the various orifices between the fan chamber and each of the cushions, between each of the cushions and the atmosphere, and between forward and aft cushions. The continuity equation specifies that the sum of the

input flow to a cushion, the output flow, and the gains or losses due to compressibility must equal zero. The equation of continuity for the forward cushion is

$$Q_{e1} - Q_{i1} + Q_{m1} - Q_{w1} + Q_{e3} + Q_{c1} = 0 \quad (4a)$$

and for the aft cushion

$$Q_{e2} - Q_{i2} + Q_{m2} - Q_{w2} - Q_{e3} + Q_{c2} = 0 \quad (4b)$$

where Q_{i1} and Q_{i2} are the inlet flows from the fan chamber, Q_{e3} is the stability skirt flow between the cushions, Q_{e1} and Q_{e2} are escape flows through forward and aft skirts, Q_{m1} and Q_{m2} are the air flows associated with changes in cushion volume due to craft motion, Q_{w1} and Q_{w2} are the air flows resulting from volume changes arising from varying terrain, and Q_{c1} and Q_{c2} are effective air flows associated with air compressibility effects and the rate of change of density of the cushion fluid.

The relationship between pressure and air flow through various openings is specified by the general orifice equation

$$Q = C_{D_i} A_i \sqrt{2\Delta P / \rho} \quad (5)$$

where C_{D_i} is an orifice discharge coefficient associated with orifice area A_i , and ΔP is the pressure difference across the orifice.

The discharge coefficients used in the present analysis have been derived from experimental studies currently underway. Geometrical data were obtained directly from the 1:12 scale JEFF(B) model used in the validation experiments. Orifice areas consisted of a large number of small orifices of various shapes. The measured leakage area represented a lower bound since small leakage areas could not be accurately measured.

The escape areas under the skirts and the stability seals are calculated by integrating the gap between the bottom of the skirt and the supporting surface under the skirt perimeter. The resulting leakage area depends upon the craft motion and craft orientation, which are computed in the motion simulation, and also upon the terrain geometry relative to the ACV. The analytical model for the leakage gap employed in the simulation results presented in this report is given by

$$l(x, z, t) = z + x\theta - h_k(x) - z_w(x + Ut) \quad (6)$$

where h_k is the skirt height, z_w is the terrain profile, U is the craft velocity, and θ is the pitch angle which has been assumed to be small. The small angle approximation is appropriate since predicted pitch angles are typically less than 6 degrees. A negative value for l indicates that the skirt is in contact with the surface, i.e., there is no gap, in which case l is set to zero. In order to handle the case in which $l < 0$, l can be written as $l' = -lH(l)$, where $H(l)$ is the Heaviside function.

AIR FLOW DUE TO CRAFT PUMPING

The craft pitch and heave motion resulting from interaction with its environment causes the volume of the forward and aft cushions to change as a function of time. The contribution to incompressible flow resulting from craft motion is assumed to be equal to the product of the craft's average vertical velocity in the chamber in question and the cross-sectional area of the forward or aft cushion, as appropriate. The craft pumping term Q_m is therefore given by

$$Q_m = \{\dot{z} + (\bar{x} - x_g) \dot{\theta}\} S \quad (7)$$

where S is the cushion cross-sectional area and \bar{x} is the location of the cushion centroid. The centroid of the cushion is assumed to be at the center of the cushion segment under examination.

AIR FLOW DUE TO TERRAIN PUMPING

The air transport effect of forward motion over fixed terrain is given for each cushion segment by

$$Q_w = \int_{L_1}^{L_2} \frac{\partial}{\partial t} z_w(x,t) B dx \quad (8)$$

where B is the craft beam, x is measured along the length of the craft, and L_1 and L_2 are the x positions of the cushion front and back boundaries. For free surface simulation this term is referred to as wave pumping and must include the celerity of the wave field.

The form of the above expression is of particular interest when the terrain has a simple trigonometric profile since arbitrary profiles can always be represented by a suitable Fourier series. If the terrain, z_w , is given by

$$z_w(x,t) = a \cos(k_w x + \omega t) \quad (9)$$

and the integration occurring in the expression for Q_w is carried out, the terrain pumping term for the bow cushion becomes

$$Q_{w1} = \frac{a B \omega}{k_w} \{ (\cos k_w L/2 - 1) \cos \omega t - \sin k_w L/2 \sin \omega t \} \quad (10a)$$

and for the aft cushion

$$Q_{w2} = \frac{a B \omega}{k_w} \{ (1 - \cos k_w L/2) \cos \omega t - \sin k_w L/2 \sin \omega t \} \quad (10b)$$

AIR FLOW DUE TO COMPRESSIBILITY OR CUSHION PUMPING

The effect of the compressibility of the air in the cushion of the ACV can be represented to first order in time rate of change of density by an air flow term given by

$$Q_c = V \dot{\rho} / \rho_a \quad (11)$$

where ρ is the cushion air density and ρ_a is the ambient air density. An adiabatic isentropic equation of state is employed to relate the density to the pressure in the cushion. The state equation is given by

$$1 + p/p_a = (\rho/\rho_a)^\gamma$$

where p_a is the ambient atmospheric pressure and γ is the ratio of specific heats. If the state equation is solved for $\dot{\rho}/\rho_a$ the result is

$$\dot{\rho}/\rho_a = \frac{\dot{p}}{\gamma p_a} \left(\frac{p}{p_a} \right)^{\frac{1-\gamma}{\gamma}} \approx \frac{\dot{p}}{\gamma p_a}$$

where the last expression is obtained by neglecting terms of the order,

$$\frac{(1-\gamma)}{\gamma} \left(\frac{p}{p_a} - 1 \right)$$

The effective air flow due to compressibility, which is the true cushion pumping term Q_c , can be determined as a function of pressure by using the above expression for $\dot{\rho}/\rho_a$, resulting in

$$Q_c = V\dot{\rho}/\rho_a \approx V\dot{p}/(\gamma p_a) \quad (12)$$

SKIRT FORCES

The analytical model for the force F_v arising from skirt contact with the supporting surface is highly nonlinear even though simplifying assumptions are made in modeling the skirt geometry. It is assumed that the materials used in constructing the skirts are sufficiently flexible that restoring forces associated with the material can be neglected. It is also assumed that frictional forces arising from contact with the supporting surface do not deform the skirt in the body x direction, implying that when contact is made the skirt compresses in the vertical direction only. An illustration of the skirt deformation during contact with the supporting surface is presented in Figure 2. The vertical force associated with the supporting surface contact arises from the cushion or skirt bag air pressure acting over the surface of contact. In terms of the variables illustrated in Figure 2, the total vertical force arising from the bow skirt contact is given by

$$F_1 = P_1 B(d_2 - d_3) + 2P_f B d_3$$

where B is the skirt beam, $B(d_2 - d_3)$ is the skirt contact area, $2Bd_3$ is the skirt bag contact area, P_1 is the cushion pressure, and P_f is the skirt bag pressure which is assumed to be the same as the fan chamber pressure. The above expression can be written in terms of the skirt

height L_s and the angle α_b that the skirt makes with the vertical. The resultant force is given by

$$F_1 = P_1 B (L_s \tan \alpha_b - d_3) + 2P_f B d_3 \quad (13)$$

The distance d_3 can be obtained from the effective radius of the bow skirt bag R_c and the bow skirt deformation height ℓ'_b , hence,

$$d_3 = \{(\ell'_b - L_s) (2R_c - \ell'_b + L_s)\}^{\frac{1}{2}}$$

The aft skirt is modeled without a bag. Hence, the vertical force associated with aft skirt contact is given by

$$F_2 = (P_f - P_2) B \ell'_a \tan \alpha_a \quad (14)$$

where P_2 is the aft cushion pressure, ℓ'_a is the deformation of the aft skirt, and α_a is the angle the aft skirt makes with the vertical. The total vertical force F_v is then given by

$$F_v = P_1 B (L_s \tan \alpha_b - d_3) + 2P_f d_3 + P_2 B \ell'_a \tan \alpha_a$$

Occasionally the craft hull above the skirt bag will impact the supporting surface. When this occurs, the vertical force is replaced by a rapidly increasing function of the deformation height. The deformation of the skirts, ℓ' , can be written in terms of the mathematical expression given for ℓ in Equation (6)

$$\begin{aligned} \ell'_b &= -\ell(L/2, z, t) H(-\ell) \\ \ell'_a &= -\ell(-L/2, z, t) H(-\ell) \end{aligned} \quad (15)$$

where $H(\ell)$ is the Heaviside function.

SKIRT MOMENTS

Three different effects are considered in modeling the moments due to the skirts. These effects are the reaction phenomena arising from air escaping from the cushion under the skirt, frictional effects due to skirt contact with the supporting surface, and skirt deformation effects during skirt contact with the supporting surface. The reaction moment is given by

$$M_R = -P_1 B \ell (L/2, z, t) \{z_g + h_{k1} + \frac{1}{2} \ell (L/2, z, t)\} H(\ell) \\ + P_2 B \ell (-L/2, z, t) \{z_g + h_{k2} + \frac{1}{2} \ell (-L/2, z, t)\} H(\ell) \quad (16)$$

The seal contact moment is obtained by multiplying the seal contact forces by appropriate moment arms and summing. The results are

$$M_C = F_1 (L/2 + \frac{1}{2} \ell'_b \tan \alpha_b) + F_2 (-L/2 - \frac{1}{2} \ell'_a \tan \alpha_a) \quad (17)$$

where Equations (13) and (14) have been employed. The moment arising from frictional forces is given by

$$M_F = -F_1 \mu (h_{k1} - \ell'_b) - F_2 \mu (h_{k2} - \ell'_a) \quad (18)$$

where μ is the coefficient of friction. The total skirt moment M is given by

$$M = M_R + M_C + M_F$$

SOLUTION OF AIR FLOW EQUATIONS

The continuity equations for the forward and aft cushions given by Equation (4) can be written as functions of the unknown pressures P_1 , P_2 , and P_f by using Equations (3), (5), (8), (10), and (12). The explicit form for the resulting pressure dependent functions is not presented here, since evaluations of the functions in the computer simulation program proved more efficient.

The three-dimensional generalized Newton-Raphson numerical procedure is used to solve the resulting equations for the pressures P_1 , P_2 , and P_f required in the equations of motion. Since the equations involved do not contain very complicated expressions in terms of pressures, a more sophisticated numerical procedure is not warranted. Convergence is occasionally slow due to oscillatory roots. In these cases, convergence is accelerated by automatically initiating the iterative procedure with a priori values equal to averages of the oscillatory roots. This only occurs when the computed values are close to the solution.

The algorithm used in implementing the Newton-Raphson procedure has other features which improve convergence. The capability of decreasing the predicted refinement by a given fraction proved quite useful in eliminating a frequently encountered problem characteristic of many Newton-Raphson algorithms, namely overestimating parameter refinements. Time histories of the cushion pressures generated by the Newton-Raphson solution procedure were examined in detail for a wide variety of cases. All values for the pressures and the time rate of change of the pressures were always consistent with the corresponding craft orientation and motion variables.

EXPERIMENTAL VALIDATION OF ANALYTIC MODEL

Extensive correlation studies with experimental data were carried out in order to verify the analytical model presented in this report. A 1/12 scale model of the JEFF(B) craft was used by DTNSRDC in an experimental program in which the model was tested over a wide range of terrain types representative of obstacles that might be encountered in a realistic overland operating environment. The experiments included towing the model over solid periodic waveforms of a wide range of amplitudes, wave lengths, and encounter frequencies. The results of this experimental program are presented in Reference 7. The model was constrained in surge during the experiments used for the correlation results presented in this report and hence numerical results are presented only for pitch and heave response.

The numerical implementation of the analytic model was exercised as presented. No artificial restoring or damping coefficients were introduced, a practice that is all too common in mathematical modeling. Computed response magnitudes were not modified, and no attempt was made to adjust mean value responses. The analytic model was used in as physically pure a form as could be developed and the result is that exceptional agreement is obtained between the experimental data and the analytic predictions. The successful verification which has been obtained is essential as a demonstration of the value of the analytic model in the overall effort of research, design, and testing of air-cushion-supported vehicles.

The validation results which are presented here are shown in terms of pitch and heave transfer functions. The pitch transfer function is defined to be the pitch angle root mean square (RMS) value normalized by the wave slope, and the heave transfer function is defined to be the heave RMS value divided by the amplitude of the periodically varying terrain. The predicted response of the craft was obtained from the time domain analytical model results after steady periodic motion was reached. For the periodic waveforms modeled, this condition was always reached in less than two encounter cycles. The actual response values were obtained in terms of the RMS value of the variable in question over one cycle of the exciting force or terrain. During the simulation computations a moving average of the response was computed in order to determine equilibrium operating conditions.

Most of the experimental and analytical transfer functions in these sections are presented as a function of wave length normalized by craft length rather than as a function of speed or encounter frequency. Presentation in this manner is appropriate since the response of the craft is more sensitive to the wave length than to speed.

Figures 3 through 8 contain analytical predictions for the first harmonic transfer function for a sinusoidal excitation and the corresponding first harmonic transfer function computed from experimental data for craft motion over trapezoidal waveforms at speeds between 4 and 15 knots. As illustrated by the figures, the agreement between predicted and experimental results is exceptionally good. Such excellent agreement between analytical model predictions and experimental data has not been demonstrated previously or presented in the literature for air-cushion-

supported vehicles. Discrepancies occur only in regions where slopes are rather steep, making it difficult to carry out accurate experimental measurements. The predicted trends with respect to speed agree very well with the measured trends in these regions, and in these and all other regions the predicted results are well within the expected experimental accuracy.

General trends that are representative of the expected craft behavior are quite apparent in the analytical results presented in this report. In the long-wave-length limit, it is expected that the craft motion will be parallel to the wave surface. Consequently, both the pitch and heave transfer functions approach unity in the long-wave-length limit. As the wavelength approaches small values, the effects of the peaks and troughs under the craft tend to average out, producing no net moment or heave force. Hence in the short-wave-length limit the envelope which contains the maxima of the transfer functions should finally approach zero.

The detailed behavior of the response includes null points at integral fractions of wave-length-to-craft-length ratio. These null points arise from a resonance type of phenomenon between the cushions and the wave terrain, resulting in cancellation of contributions to the force and moment associated with bow and aft cushions and with null conditions for craft and terrain pumping terms so the null points will be sharp if the craft length is well defined. In the present analytical model for the skirts, allowance is made for craft length changes due to skirt contact with the terrain. These changes in length tend to reduce

the sharpness of the null points, an effect that is quite apparent in both the predicted results and the experimental data. This type of response behavior implies that the skirt model, although simple, is valid.

APPLICATIONS OF THE ANALYTICAL MODEL

An air cushion vehicle motions or simulation model may be employed with assurance in craft dynamics studies only after it has been thoroughly validated through correlation with experimental data. Having shown that the present ACV mathematical model performs correctly for overland operation in two degrees of freedom over rigid periodic waveforms, it is appropriate to present a brief investigation of various dynamic characteristics of the ACV. Included in this overview of dynamic response characteristics is an investigation of linearity in the pitch-heave response, an examination of the magnitude of terrain pumping terms in the mathematical model, a demonstration of the effect of modifications in the properties of the fan curve on vertical plane motion, a brief examination of the effect of compressibility of the cushion fluid, and an initial investigation of the subharmonic character of ACV overland response.

RESPONSE LINEARITY

The degree of nonlinearity in the overland response dynamics of the ACV analytical model has been investigated as a function of terrain amplitude for sinusoidal excitation over a range of encounter frequencies. The results of this investigation are presented in Figures 9 through 12.

Pitch and heave transfer functions are shown in Figures 9 and 10 as functions of wave slope for fixed values of wavelength. Results are obtained for various frequencies by changing the speed of transit over the wave field. For a linear system the transfer functions would appear as straight horizontal lines, indicating that the pitch and heave response at a given encounter frequency is directly proportional to the wave amplitude. The deviations from constant response appearing in these figures indicate the degree of nonlinearity observed at specific excitation frequencies. It is evident that for any specific excitation frequency there are regimes in which the ACV response may be classified as linear and other regions in the wave amplitude domain in which the nonlinear behavior of the vehicle is dramatic. Factor-of-two variations in the response amplitude are not uncommon for small wave slopes, but the ACV response tends to be more linear for steeper waves. It should be noted that the peaks in the pitch transfer functions shift toward larger wave amplitudes as the craft speed is decreased. It is especially important to note the manner in which the heave inflection point moves to larger wave slopes with decreasing speed. The curve presented for 46.8 knot operation (13.5 kts model scale, $F_n=1.56$) shows that the magnitude of the heave response doubles in the middle of a range of wave slopes representative of common terrain.

The predicted transfer functions are presented as functions of encounter frequency in Figures 11 and 12 for three different wave amplitudes. In this presentation, all three normalized curves would coincide for linear system response. The large differences among these

curves indicate strongly nonlinear behavior exhibited by the ACV as the wave amplitude approaches zero. Over the range of amplitude ratios (a/L) considered, the frequency associated with the pitch resonance shifts to higher frequencies for flatter terrain (i.e., smaller wave amplitudes). The peak heave resonance frequency behaves in a similar manner, moving to a higher frequency with decreasing wave slope. The implication of this behavior, in which the nonlinear character in ACV response dominates the dynamic performance for the flatter terrain, is disturbing since it is under these conditions that one expects linear theory to be applicable. Fortunately the concern is only academic since the actual ACV response is minimal.

TERRAIN PUMPING

The expression "terrain pumping" refers to changes in the cushion air flow due to motion of the craft over terrain of varying elevation. For a sinusoidal terrain, the terrain pumping effect results in a sinusoidal air flow term (Q_w) in each cushion. When the bow and aft cushion discharges are in phase or additive, the heave response is magnified. Likewise, whenever the changes in bow and aft cushion are out of phase, the pitch response will be most affected. The time-average of the sum and difference of the two flows is shown in Figure 13. Examination of the flows shows that the difference peaks at a wave-to-cushion-length ratio of 1 ($\lambda/L=1$) and has a null point at the half craft length ($\lambda/L=0.5$) while the sum peaks at a wave-to-cushion-length ratio of 2 ($\lambda/L=2$) and has a null point at unity ($\lambda/L=1$). This phenomenon explains the appearance of null points in the pitch and heave response but since both pitch and heave are strongly coupled, the maximum responses are expected to occur at

wave-to-cushion-length ratios shifted somewhat from these integer values. This is quite evident from the transfer function results presented in Figures 4 through 8.

Other factors also determine where the maxima and minima will occur. Among these are the resonant response of the craft in pitch and heave and the interaction of the skirts with the supporting surface. This interaction results in a speed-dependent minimum in the heave response at a wave-to-cushion-length ratio of 1.3 for a full-scale JEFF(B) speed of 27.7 kts ($F_n=0.93$) and at about 1.1 for a speed of 52 kts ($F_n=1.74$). This result may be interpreted as follows. The contact forces given by Equations (13), (14), (16), (17), and (18) are highly nonlinear and thus can be expected to shift the minimum response point away from unity. Since the wave pumping term increases linearly with speed or encounter frequency, it would tend to dominate the response at higher speeds. It is observed in Figures 6 and 8 that the heave minimum is closer to a reduced frequency of 1 at 52 kts ($F_n=1.74$) than it is at 27.7 kts ($F_n=0.93$).

LIFT FAN CHARACTERISTICS

It is important in the design of an ACV lift system to determine the effects that various fan characteristic curves will have on the dynamic performance of an ACV. The present ACV analytical model may be employed to parametrically investigate lift system and fan flow modifications. Two numerical experiments have been performed: changes in the total flow (ϕ) at a given pressure (ψ) and changes in the slope ($d\psi/d\phi$) of the pressure-flow curve at the mean operating point. The fan maps used

in these simulations are shown in Figure 14 and the dynamic response characteristics associated with the fan variations are shown in Figures 15 and 16. The response characteristics should be compared with the response resulting from the nominal fan performance curve. The major change in the pitch response occurs for a decrease in the lift system discharge for which the resonant point is found to increase in magnitude and move to a lower frequency. Increasing the slope of the fan map tends to flatten the pitch response and also shift the peak response to a lower frequency.

Modifications in fan performance may be expected to affect heave response more than pitch, and it is found that the heave response to modifications in fan discharge is roughly opposite that of the pitch response. As the flow is increased the magnitude of the heave response increases at frequencies higher than the resonant frequency, while at frequencies below the resonance range there is almost no change in response. Finally, there appears to be practically no effect on heave response when the fan slope $d\psi/d\phi$ is increased.

SUBHARMONIC OSCILLATIONS

Oscillations in pitch and heave at frequencies lower than the encounter frequencies are predicted by the analytical model. The presence of subharmonic oscillations is quite evident in the pitch and heave time histories presented in Figure 17. This subharmonic activity arises from the nonlinear character of the analytical model.

Half harmonic oscillations in both pitch and heave begin at nondimensional or reduced frequencies higher than 7.0 for a terrain wave

amplitude (a/L) ratio of .02 and a wave-to-cushion-length ratio of 1.65. The magnitude of the subharmonic oscillations increases to a maximum at a reduced frequency of 8.3 and decreases to a negligible value at a reduced frequency of 12. At a smaller wave amplitude ratio ($a/L = .01$), subharmonic oscillations do not appear in the reduced frequency range considered (0 to 15) in the present investigation. However, when the ambient atmospheric pressure is reduced to 0.08 atm additional subharmonics occur, ranging from the $1/3$ to $1/5$ subharmonics. These additional subharmonics are attributed to compressibility effects which are significant at reduced pressures. At some encounter frequencies the simulation times were not long enough to reach steady periodic motion in pitch or heave. This occurred at the points in the encounter frequency spectrum where the response oscillation contained more than one subharmonic or when the dominant oscillations were undergoing a transition from one predominant subharmonic to another.

CUSHION COMPRESSIBILITY

Compressibility of the cushion fluid appears to have a minor effect on model scale response at normal ambient (atmospheric) pressure. However, the compressibility effect for model scale predictions at a lower ambient pressure (over-pressure), corresponding to an equivalent full-scale operating environment, can be significant. The response of the craft at normal atmospheric pressure is compared with craft response at 0.08 atm in Figures 18 and 19. At the lower ambient pressure the effects of subharmonic oscillations are significant in the range of wave-to-cushion-length ratios between 1.5 and 2.5 ($1.5 \leq \lambda/L \leq 2.5$), as

indicated by the occurrence of a double peak at the lower pressure. For the normal pressure case the lowest harmonic predicted is at the encounter frequency. The appearance of a secondary peak for 0.08 atm over-pressure may be attributed to changes in the subharmonic response. The predominant subharmonic response is due to the $1/2$ harmonic throughout the first peak for both heave and pitch and the $1/3$ harmonic for the second peak.

Limited analytical results for over-pressures of 0.05 and 0.033 atm predict a greatly enhanced response. The main resonance peak magnifications in the heave and pitch transfer functions are as high as 10 in certain cases. These results are not presented here since the goal of the examination of cushion compressibility is the prediction of full-scale ACV response. Other components of the ACV dynamic system will be modified in the continuing examination of scale effects in order to assess the exact nature of the effect of cushion fluid compressibility.

CONCLUSIONS

A successful analytical model has been developed to predict the nonlinear pitch and heave response of an air-cushion-supported craft. The time-domain analytical model is appropriate for predicting the dynamic response during overland operation. Although the analytical model is quite general, the motion predictions have been presented for an ACV configuration that is a suitable representation for the AALC Program JEFF(B) craft.

The predicted results obtained for both pitch and heave transfer functions over a complete range of operating conditions are compared with available experimental data. The excellent correlation of the results establishes the accuracy of the analytical model and demonstrates its usefulness as a research and development tool. To this end, various parametric sensitivity studies have been conducted to explore the effects of response nonlinearity, cushion fluid compressibility, and variations in fan performance. The result of the linearity investigation indicates that the predicted pitch and heave transfer functions have regimes of linear and nonlinear behavior as functions of craft speed, amplitude, and wave length of the encountered wave-field. In general, the nonlinearities appear to dominate for small wave slopes (approaching zero) and high speeds.

Cushion fluid compressibility effects appear to be minor for a model-scale craft. However, when ambient pressures are reduced significantly in order to effectively model a full-scale cushion, the effect of gas compressibility tends to enhance the pitch and heave

response. Fairly large (approximately 15 per cent) parameter variations in the analytical fan model can be tolerated without an appreciable degradation in predicted craft dynamic performance. This apparent lack of sensitivity to fan model changes indicates that fan system parameter optimization to decrease power requirements may be a possibility.

RECOMMENDATIONS

The present analytic model has been verified on a model scale through an exceptionally successful correlation between numerical and experimental response functions. Based on these results it is recommended that the following investigations be initiated.

- (1) Extend the simulation model for full-scale JEFF(B) characteristics and perform full-scale predictions.
- (2) Extend the model to include the cushion pressure gradient. Since the predicted effects of gas compressibility proved more significant for an effective full-scale craft than for the model, it is expected that the pressure gradient associated with air flow in the cushion may have a major influence on full-scale craft response.
- (3) Extend the model to include the capability of predicting motion in all six degrees of freedom.
- (4) Perform additional parameter optimization studies, especially for lift system performance.

- (5) Apply the predictive analytical model to the AALC Program JEFF(A) craft.
- (6) Examine the function and efficiency of proposed vertical plane control devices and procedures. Investigations of this type are meaningful only if performed on a fully validated mathematical model.

REFERENCES

1. Kaplan, Paul, James Bentson, and Theodore P. Sargent, "A Study of Surface Effect Ship (SES) Craft Loads and Motions, Part 1 - Equations of Motion of SES Craft with Six Degrees of Freedom," Oceanics, Inc. Report No. 71-84A (Aug. 1971); Kaplan, Paul, James Bentson, and Theodore P. Sargent, "Advanced Loads and Motions Studies for Surface Effect Ship (SES) Craft, Part 1 - General Development of Modified Mathematical Model," Oceanics, Inc. Report No. 73-97A (June 1973); Kaplan, Paul, James Bentson, Mark N. Silbert and Howard Jaslow, "Correlation of Computer Simulation for SES Model Test Data (FY '75 Loads and Motions Studies)," Oceanics, Inc. Report No. 75-118D (Sept. 1975).
2. Doctors, L.J., "The Hydrodynamic Influence on the Nonlinear Motion of an Air-Cushion Vehicle over Waves," Proceedings of the Tenth Symposium on Naval Hydrodynamics, Office of Naval Research, Washington, D.C. (1974).
3. Lavis, D.R., R.J. Bartholomew, and T.C. Jones, "On the Prediction of Acceleration Response of Air Cushion Vehicles to Random Seaways and the Distortion Effects of the Cushion Inherent in Scale Models," AIAA/SNAME/USN Advanced Marine Vehicles Meeting (July 1972).
4. Moran, David D., and Richard S. Schechter, "The Vertical Motion of an Air Cushion Vehicle and the Spatial Distribution of Cushion Pressure," DTNSRDC Ship Performance Department Report No. SPD-615-02 (April 1976).
5. Moran, David D., James A. Fein, and Joseph J. Ricci, Jr., "The Seakeeping Characteristics of a High Length-to-Beam Ratio Surface Effect Ship," AIAA 76-862, AIAA/SNAME Advanced Marine Vehicles Conference (Sept. 1976).
6. Moran, David D., T. Michael Pemberton, and Kenneth S. Knight, "A Preliminary Experimental Investigation of the Overland Behavior of the JEFF(B) Amphibious Assault Landing Craft," DTNSRDC Ship Performance Department Report No. SPD-615-01 (June 1975).

7. Moran, David D., "The Overland Vertical Plane Dynamic Response of the AALC JEFF(B) ACV, Model Experiments," DTNSRDC Ship Performance Department Report No. SPD-615-04 (June 1976).
8. Schneider, J., and P.S. Bono, "A Study of the Dynamics of Arctic Surface Effect Vehicles: Final Technical Report, Part II: Development of the ASEV Motions Program and the Analysis of Results of Numerical Studies for Selected Craft Configurations", Oceanics, Inc. Report No. 73-101B (February 1974).
9. Bell Aerospace, "Arctic SEV Program Final Report: Volume 4, Vehicle Dynamics", Bell Aerospace, Report No. 7416-950001 (February 1973).

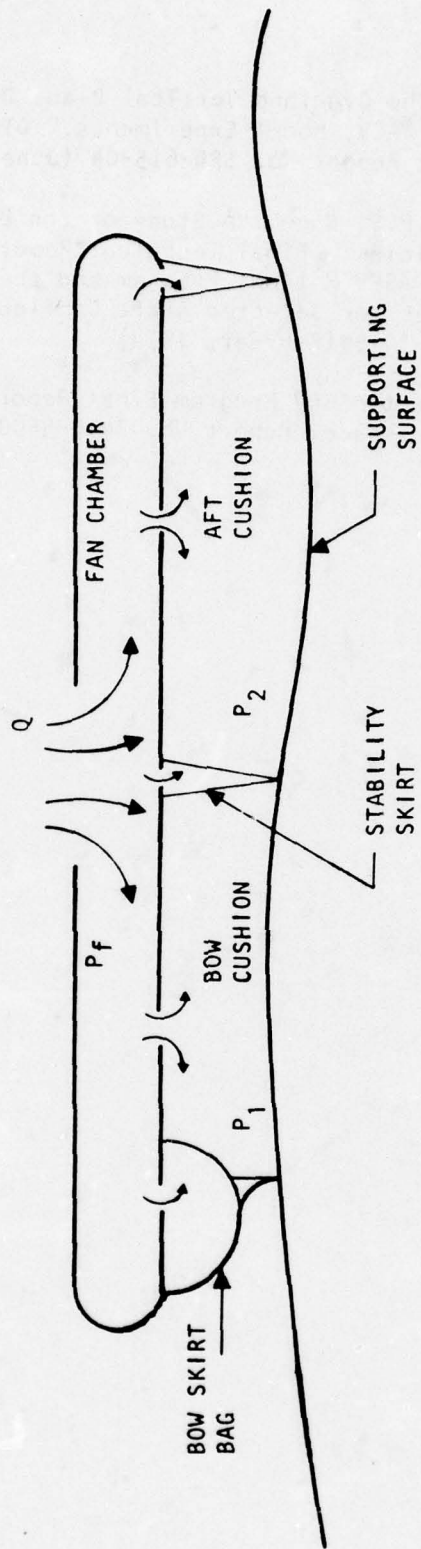


Figure 1 - JEFF(B) Lift System Configuration

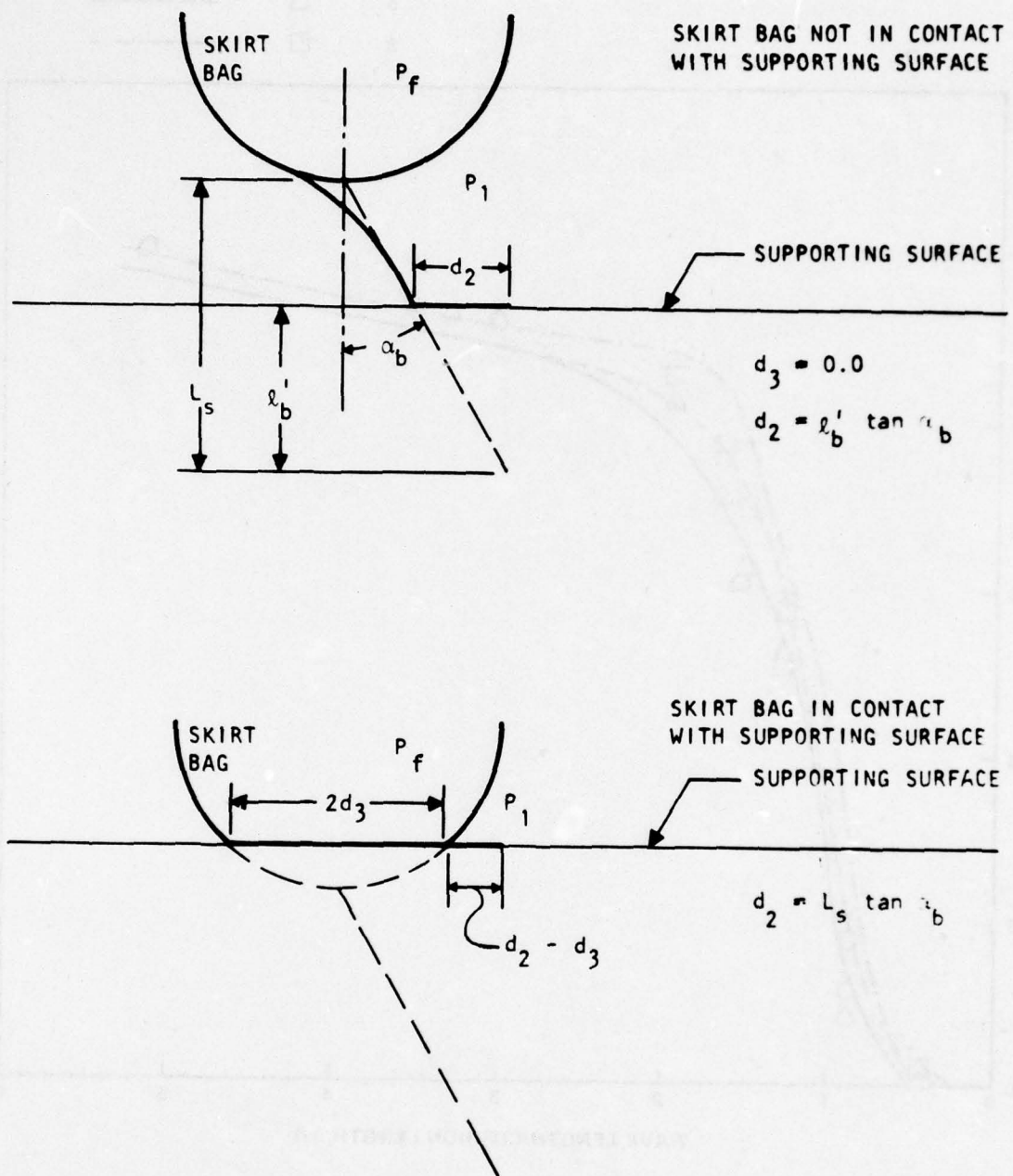


Figure 2 - Bow Skirt Configuration Employed in Analytical Model

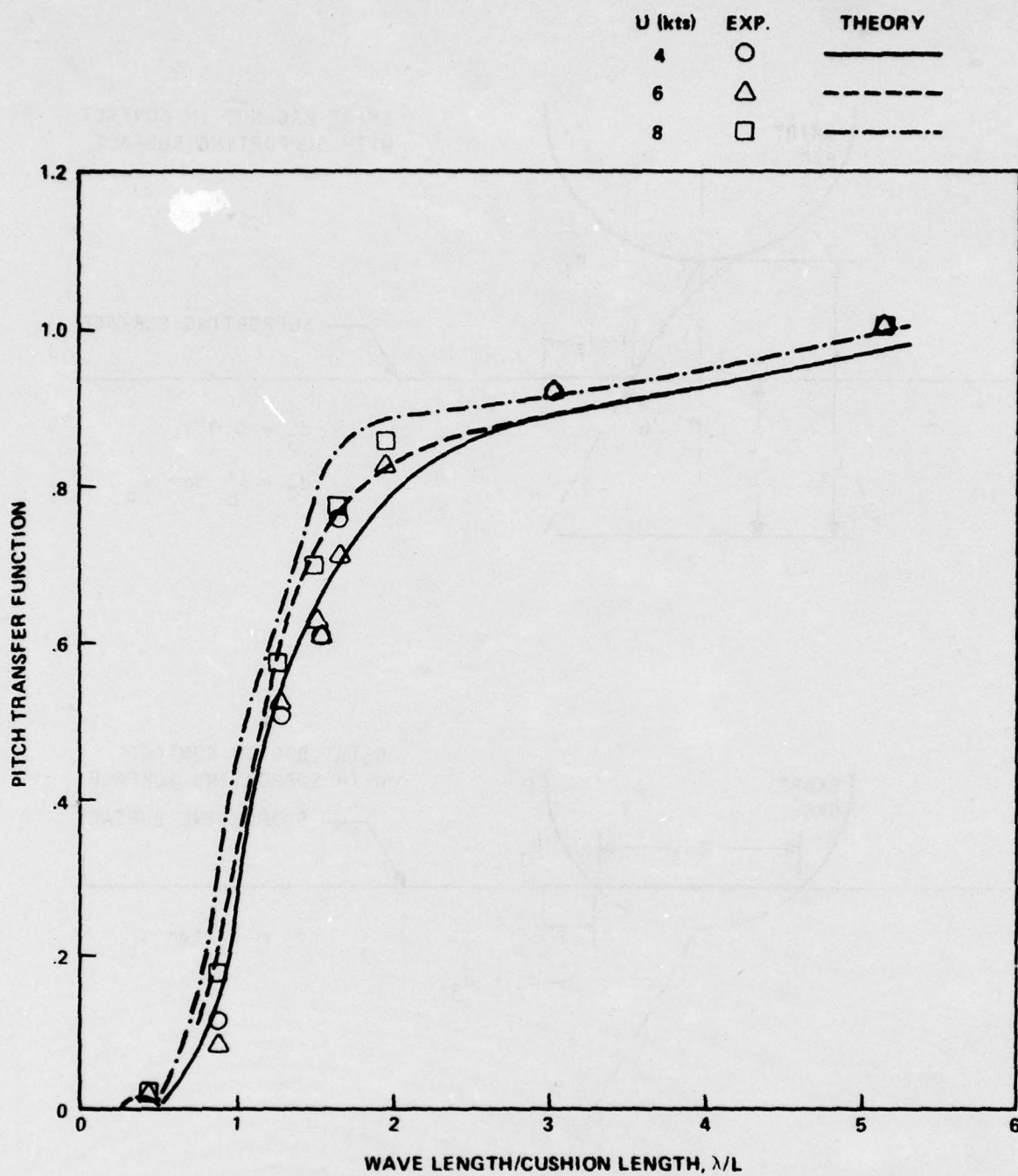


Figure 3 - Correlation of Theoretical Pitch Transfer Function with Experimental Data as a Function of Wave Length for Model Speeds of 4, 6, and 8 Knots

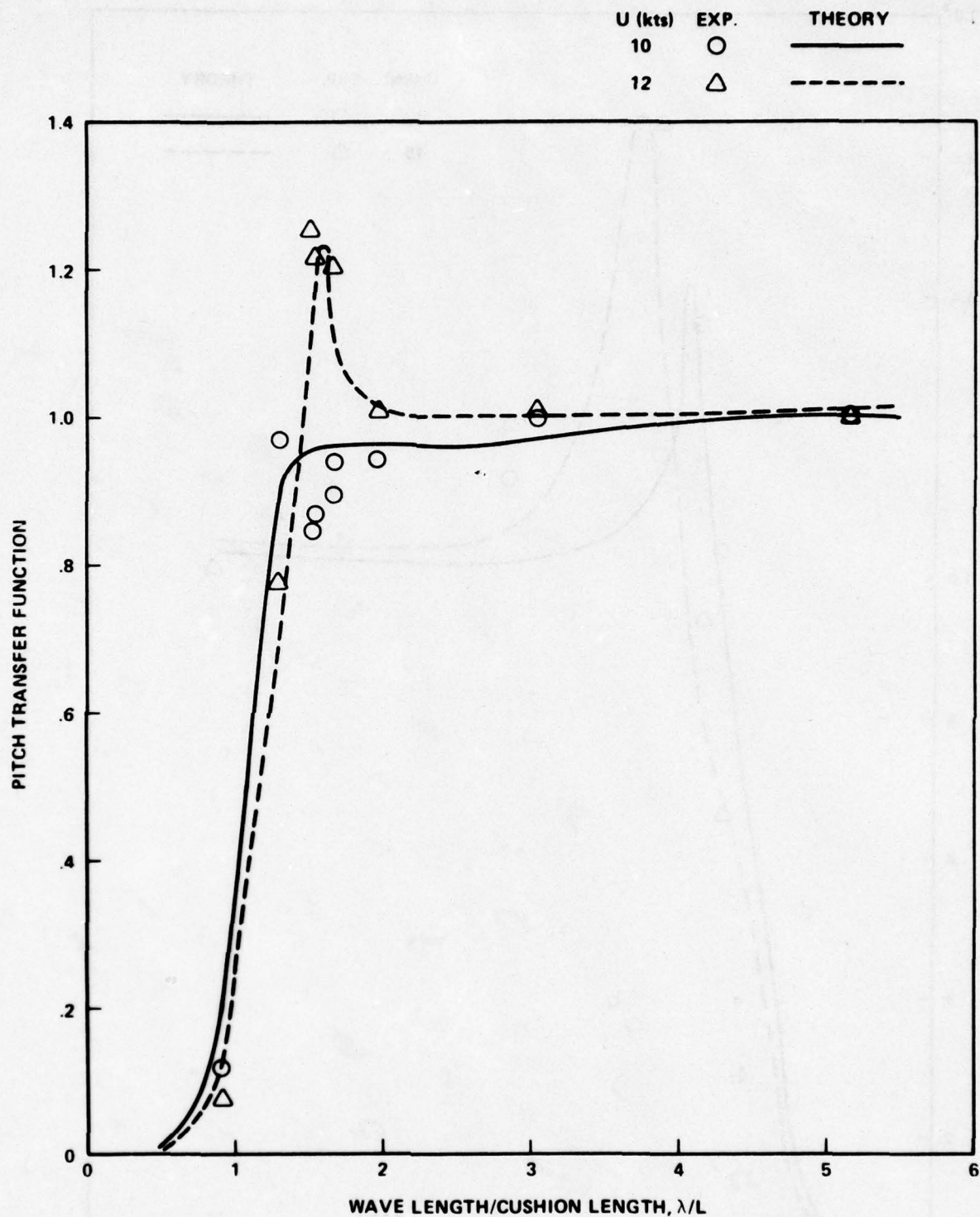


Figure 4 - Correlation of Theoretical Pitch Transfer Function with Experimental Data as a Function of Wave Length for Model Speeds of 10 and 12 Knots

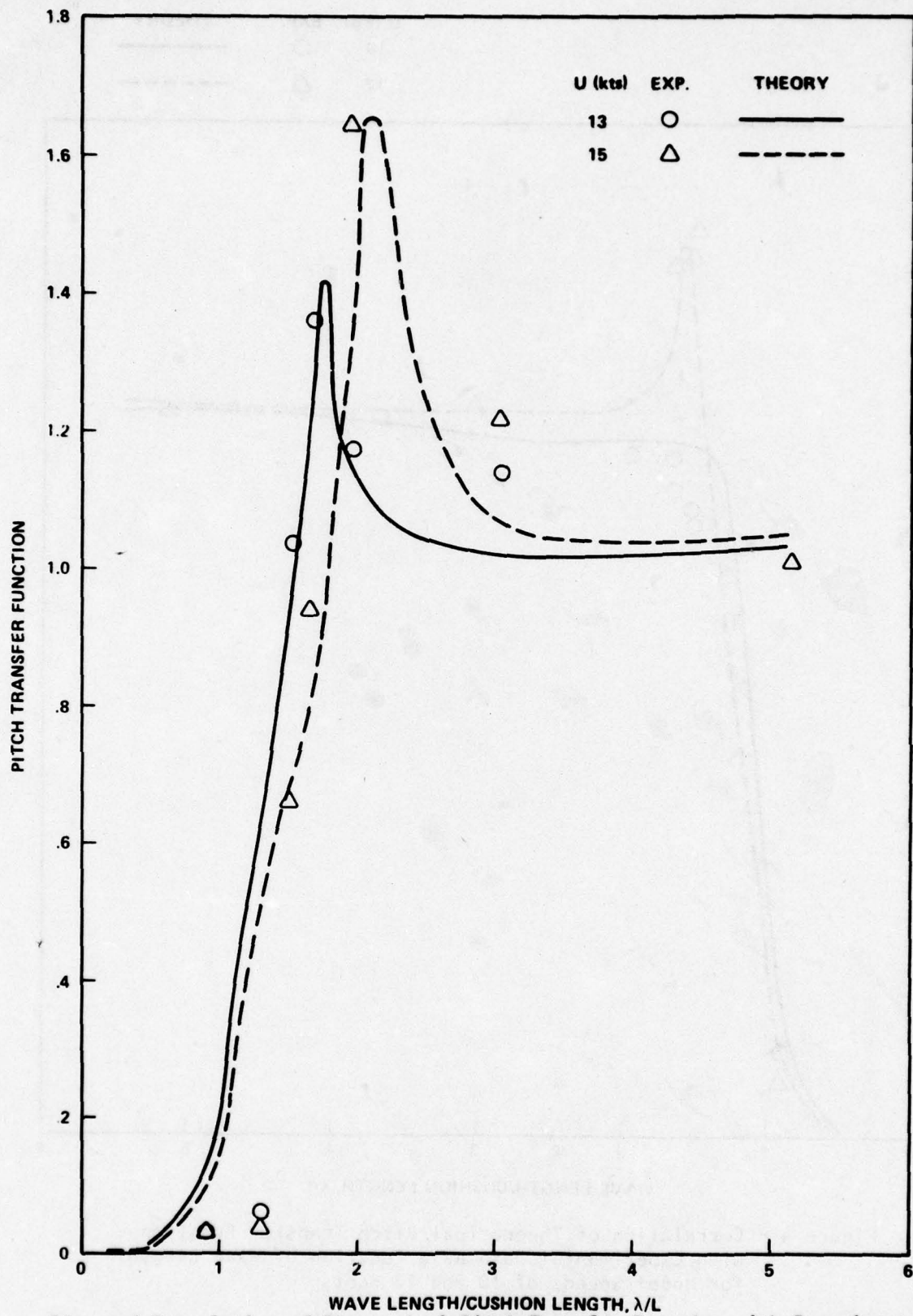


Figure 5-Correlation of Theoretical Pitch Transfer Function with Experimental Data as a Function of Wave Length for Model Speeds of 13 and 15 Knots

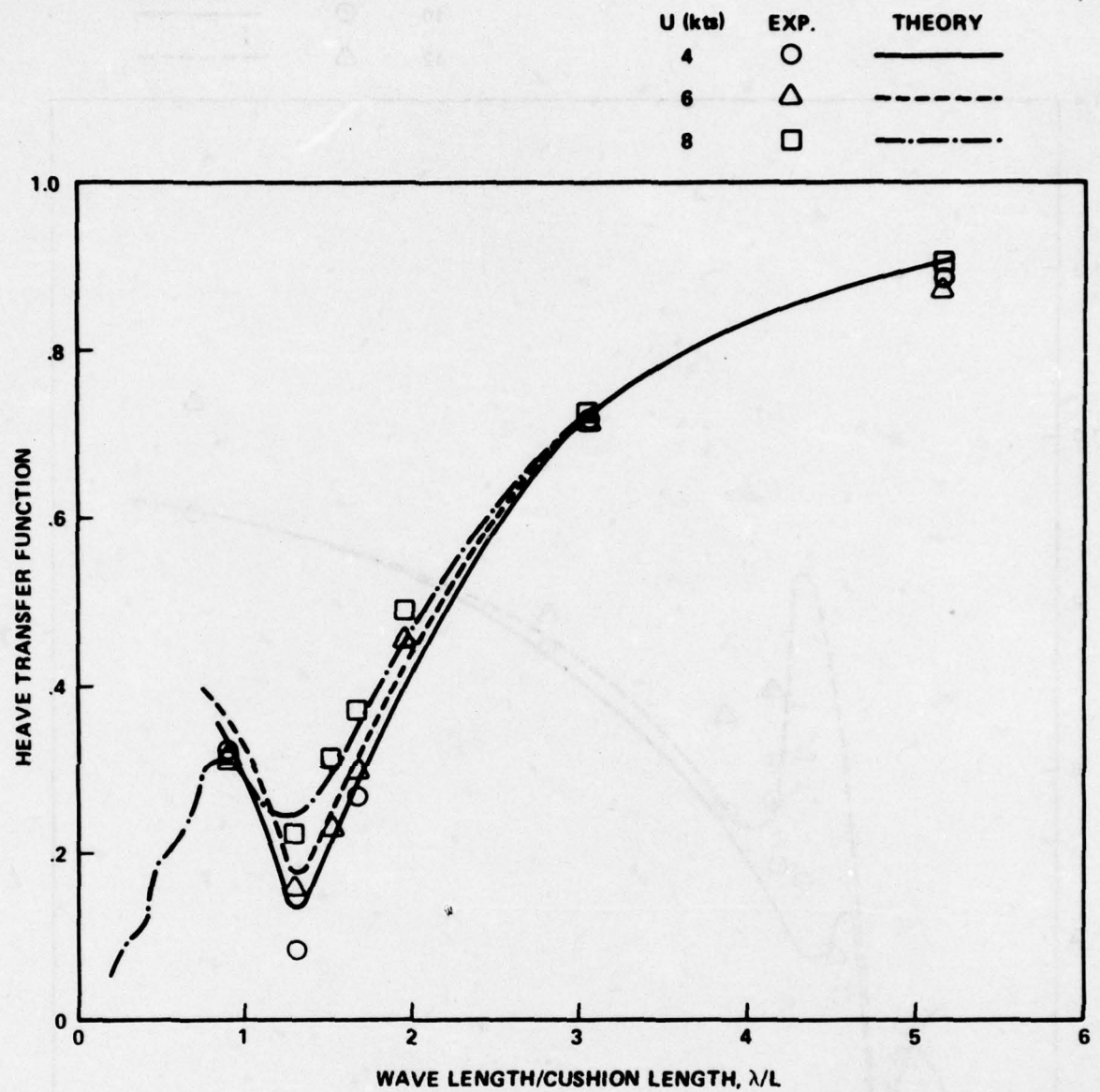


Figure 6 - Correlation of Theoretical Heave Transfer Function with Experimental Data as a Function of Wave Length for Model Speeds of 4, 6, and 8 Knots

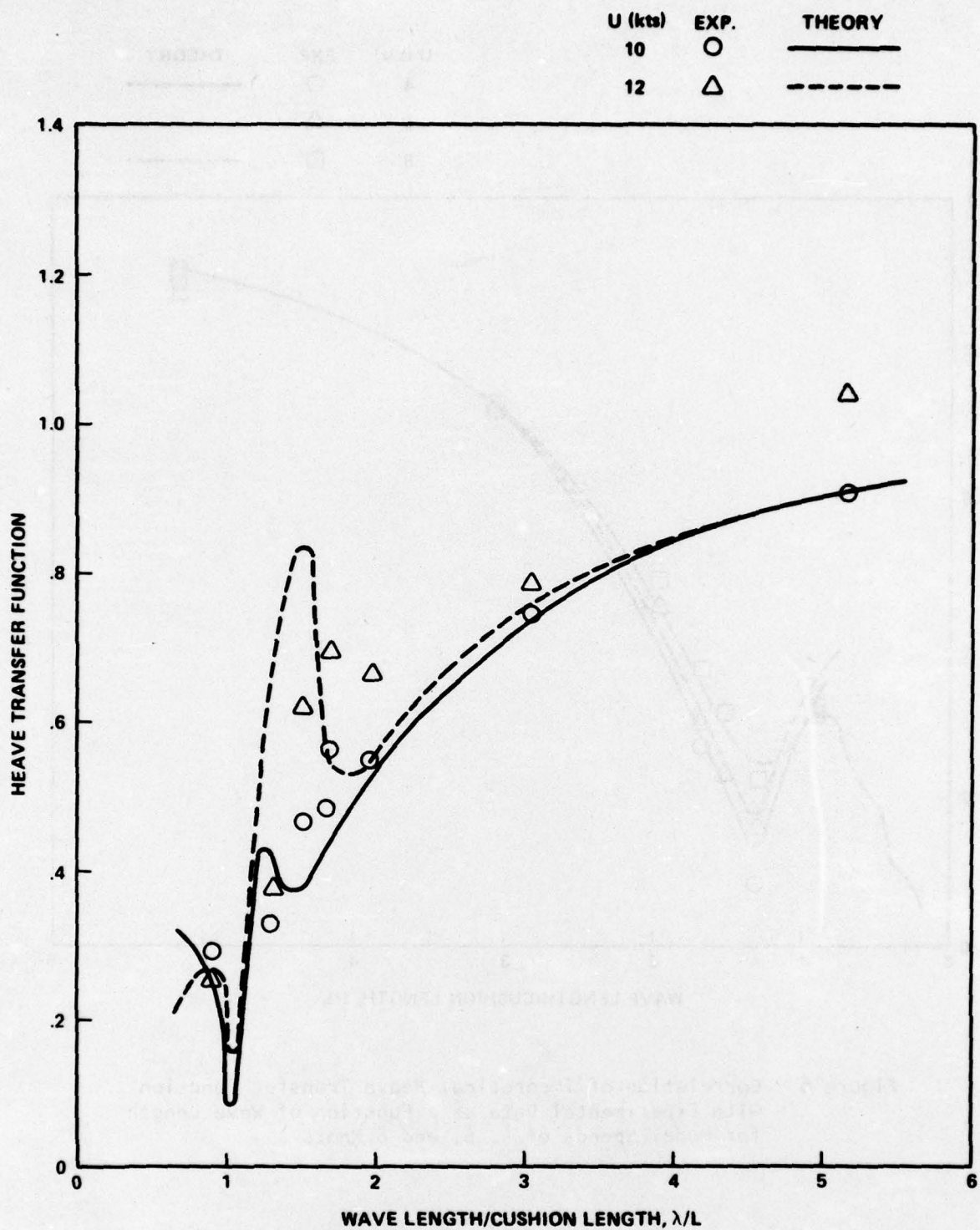


Figure 7 - Correlation of Theoretical Heave Transfer Function with Experimental Data as a Function of Wave Length for Model Speeds of 10 and 12 Knots

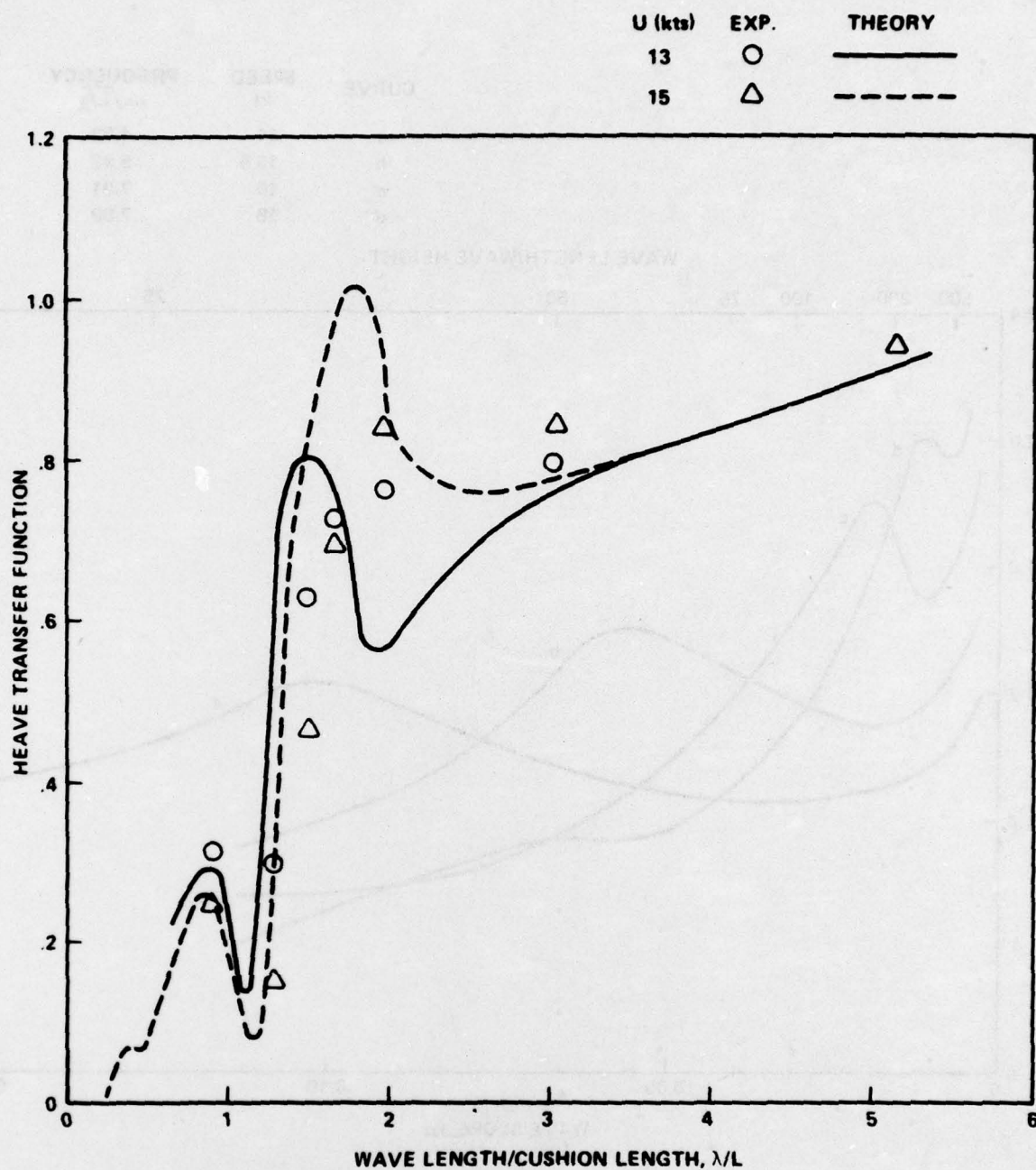


Figure 8 - Correlation of Theoretical Heave Transfer Function with Experimental Data as a Function of Wave Length for Model Speeds of 13 and 15 Knots

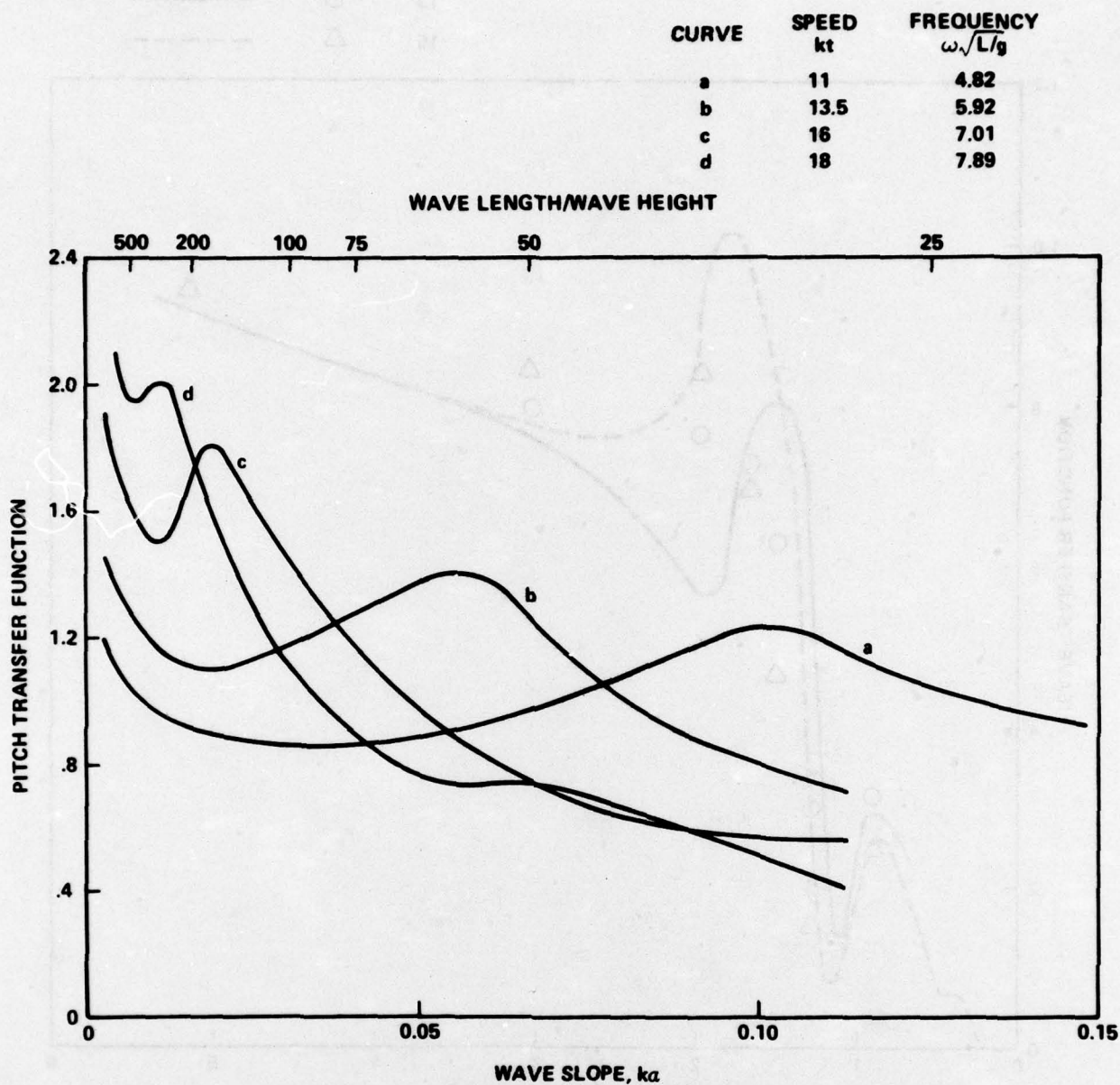


Figure 9 - Response Linearity: Pitch Transfer Function as a Function of Wave Slope for Model Speeds of 11, 13.5, 16, and 18 Knots

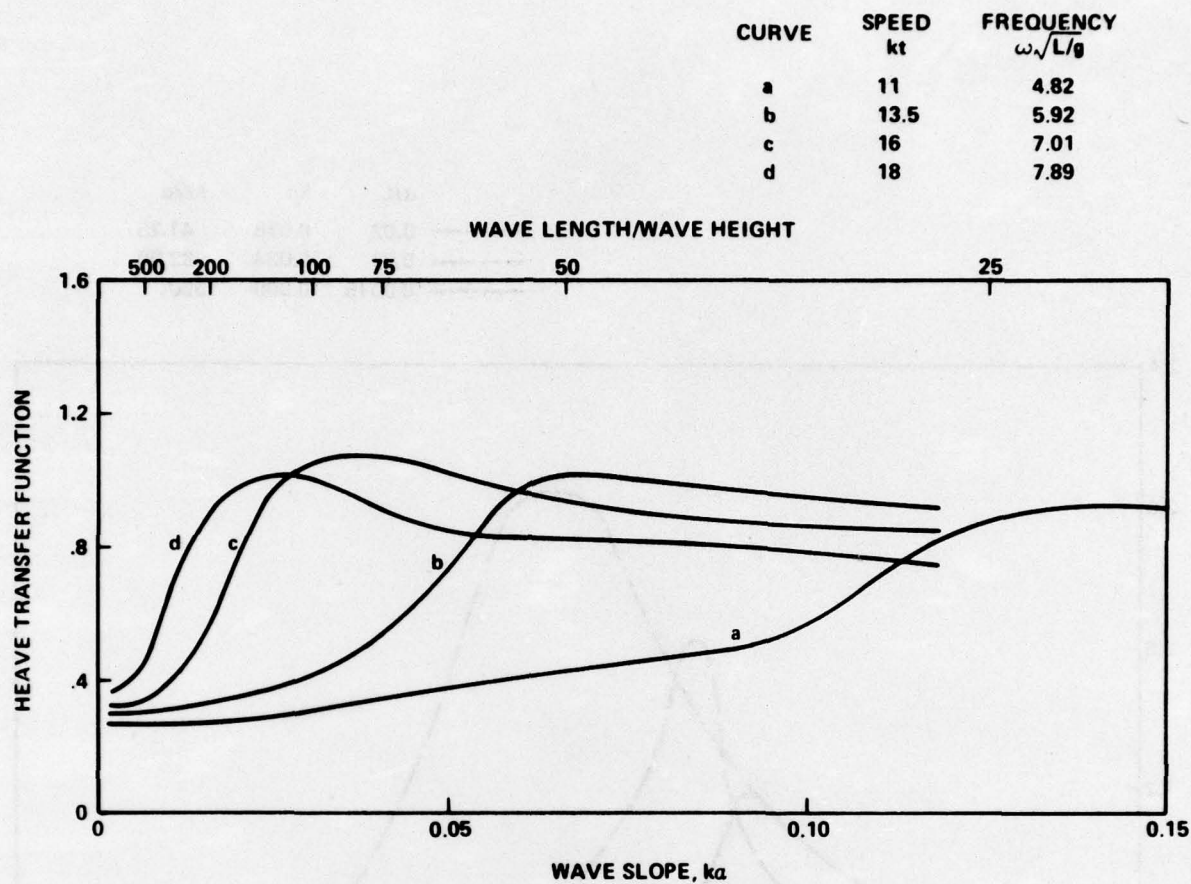


Figure 10 - Response Linearity: Heave Transfer Function as a Function of Wave Slope for Model Speeds of 11, 13.5, 16, and 18 Knots

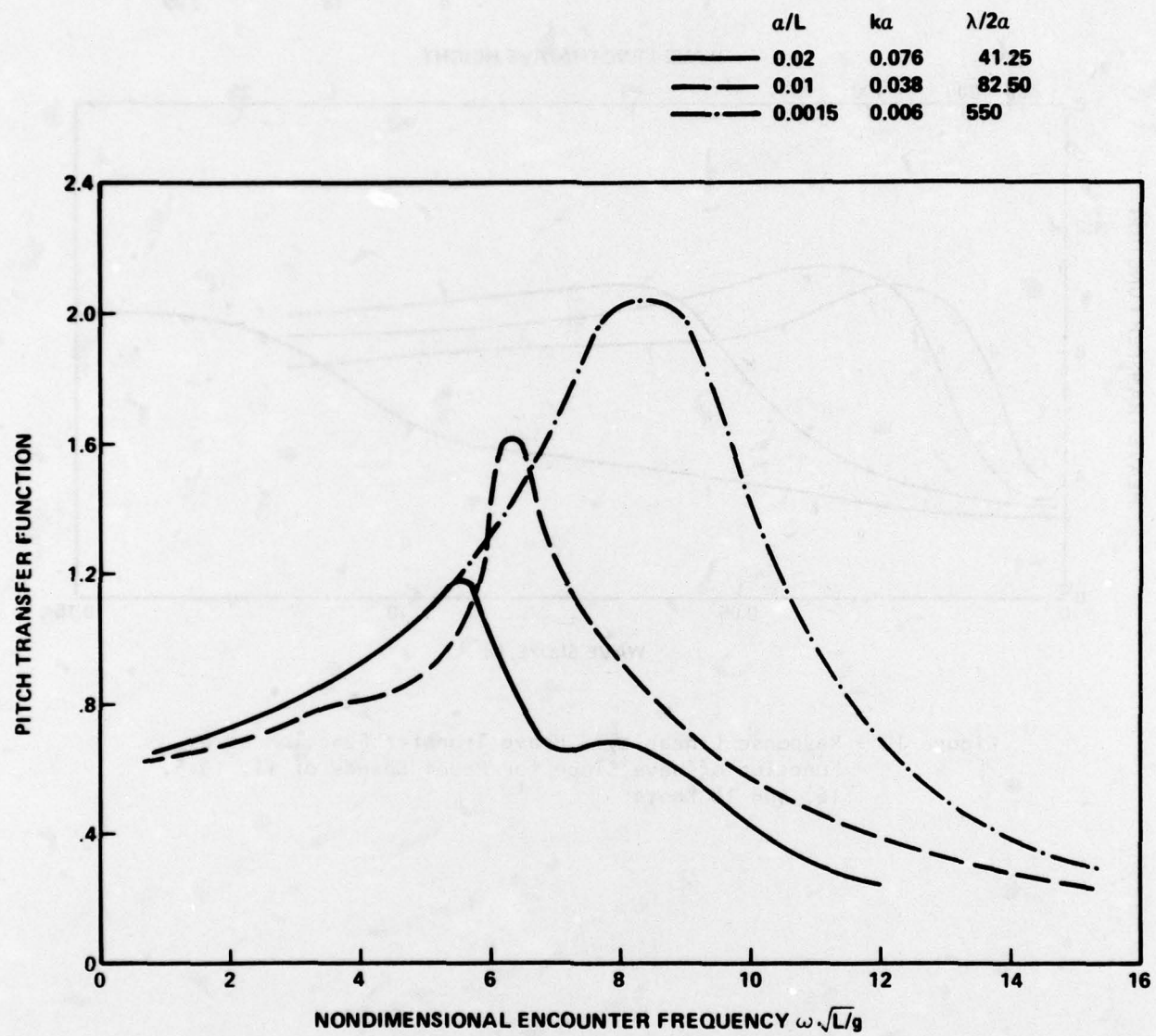


Figure 11 - Response Linearity: Pitch Transfer Function as a Function of Nondimensional Encounter Frequency for $\lambda/L = 1.65$

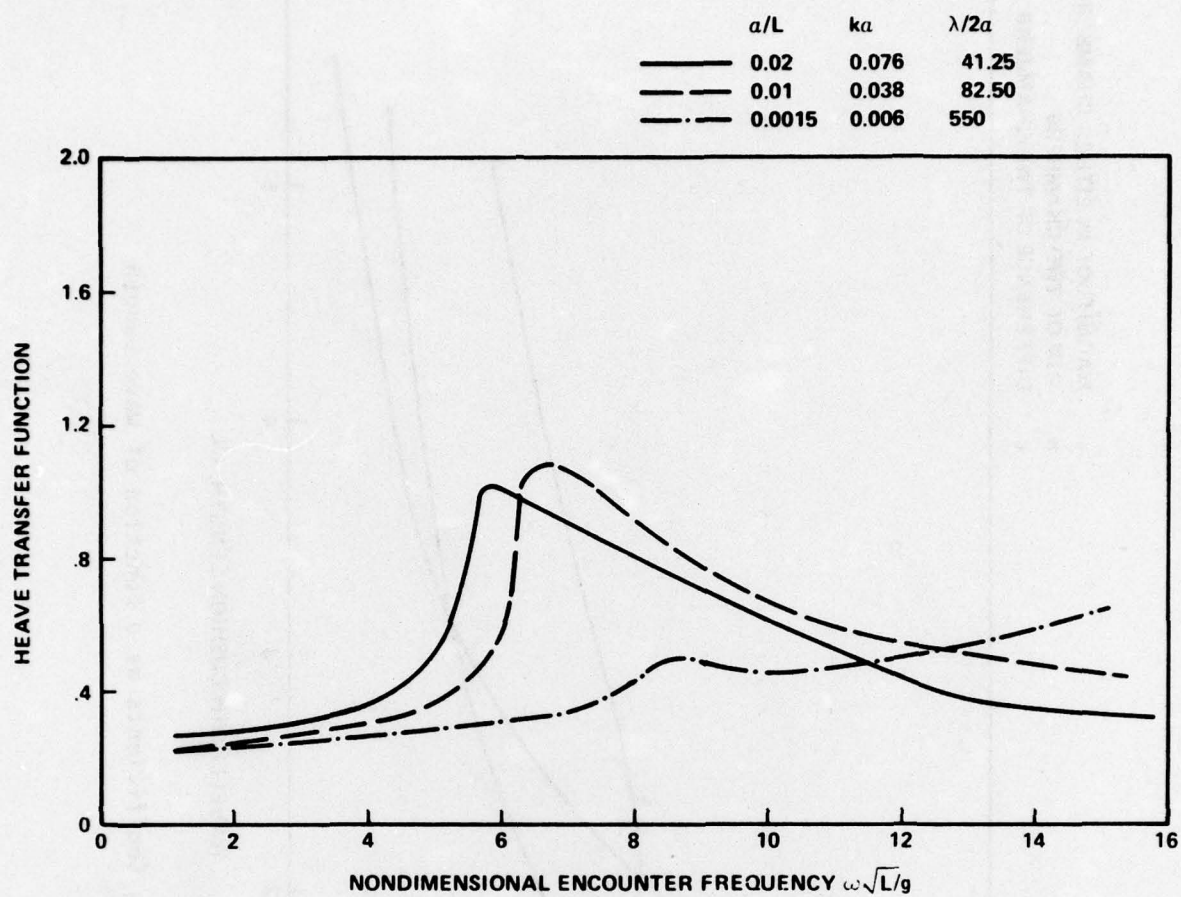


Figure 12 - Response Linearity: Heave Transfer Function as a Function of Nondimensional Encounter Frequency for $\lambda/L = 1.65$

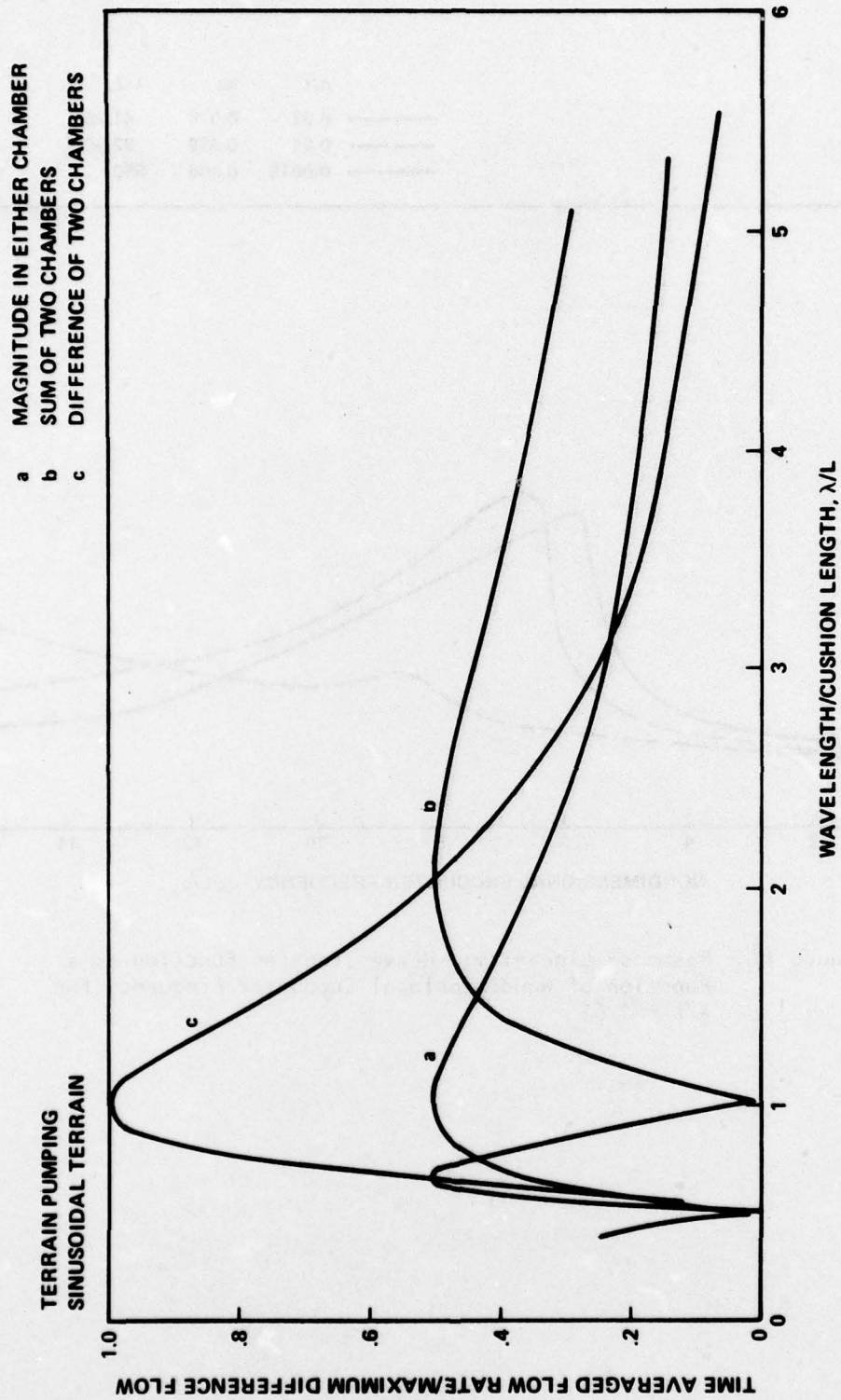


Figure 13 - Terrain Pumping Coefficients as a Function of Wave Length

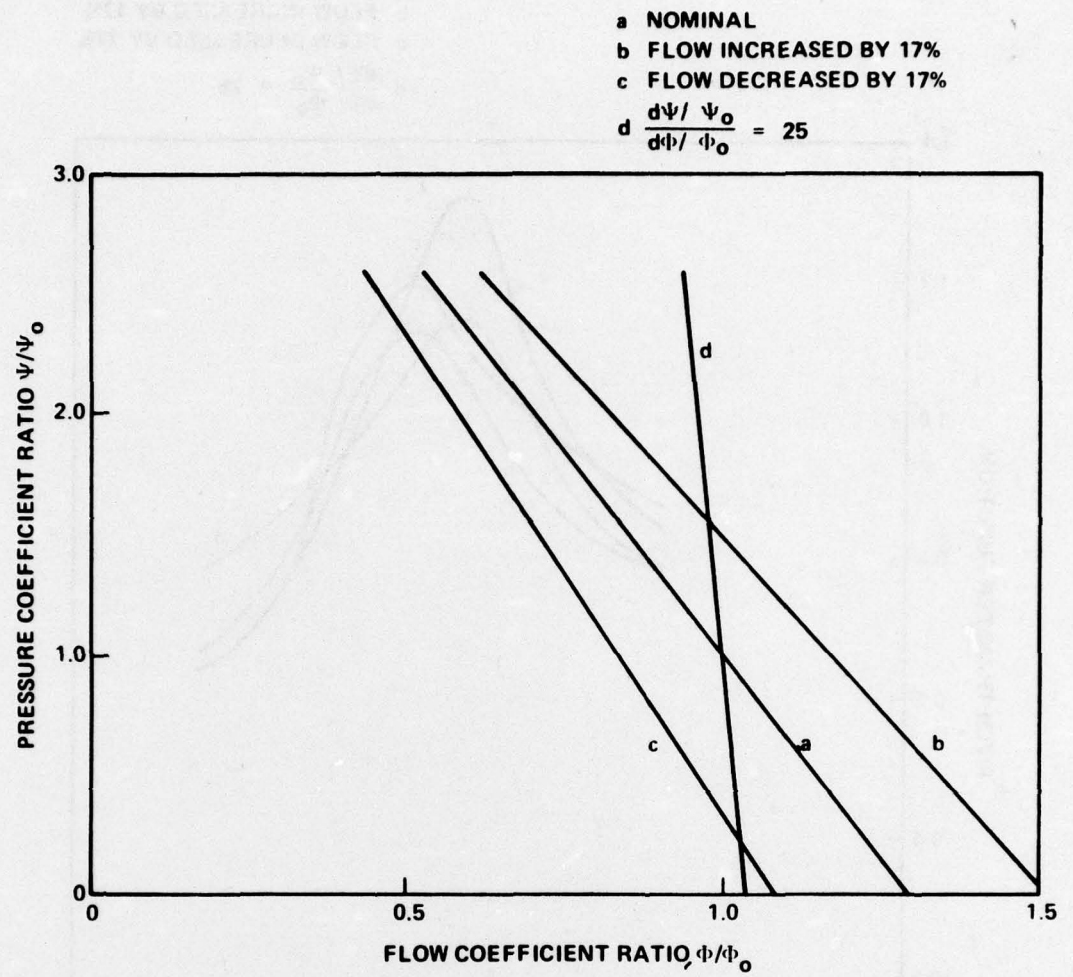


Figure 14 - Fan Performance Curves Used in Parametric Study of Lift Fan Characteristics

$$a/L = 0.02$$

a NOMINAL

b FLOW INCREASED BY 17%

c FLOW DECREASED BY 17%

$$d \frac{d\psi/\psi_0}{d\phi/\phi_0} = 25$$

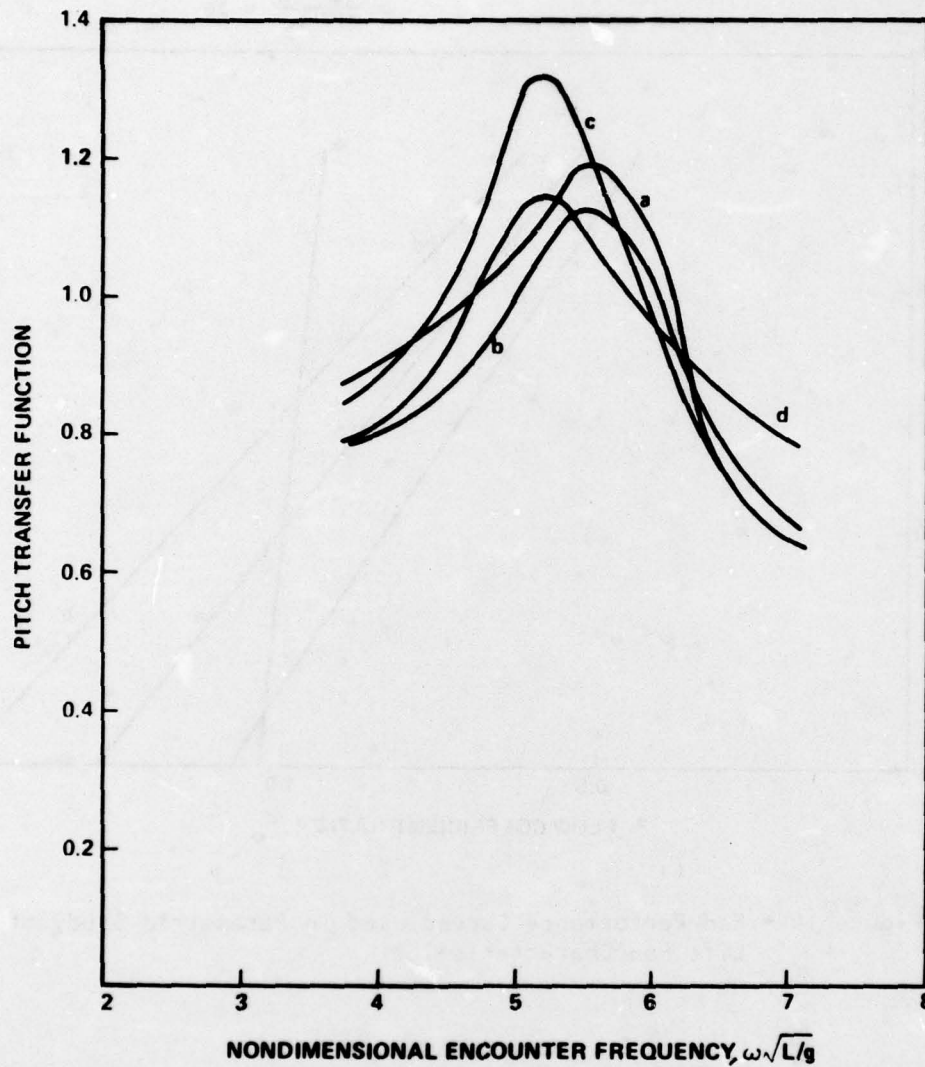


Figure 15 - Parametric Study of Lift Fan Characteristics:
Pitch Transfer Function as a Function of Encounter
Frequency for Various Fan Maps with $\lambda/L = 1.65$

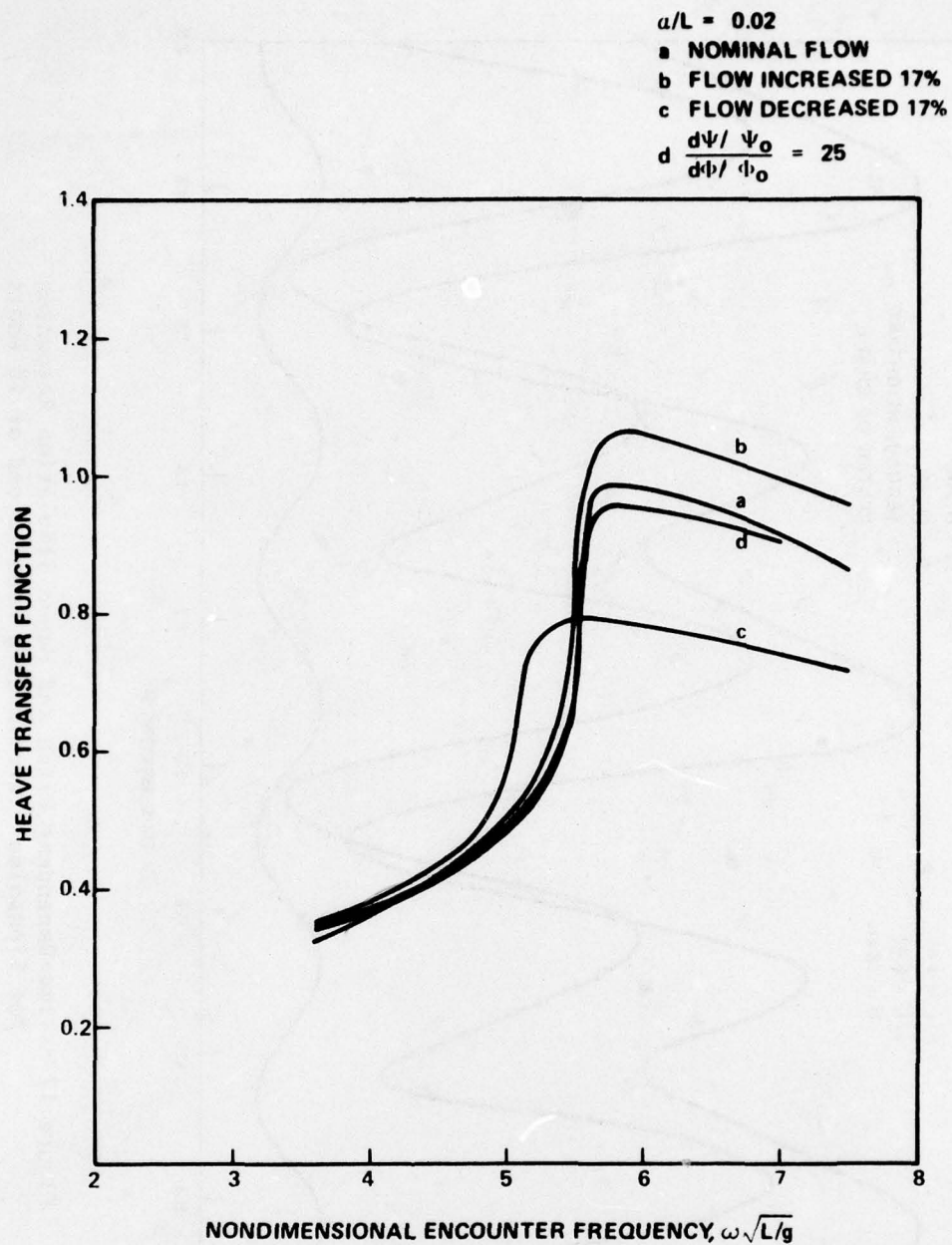


Figure 16 - Parametric Study of Lift Fan Characteristics: Heave Transfer Function as a Function of Encounter Frequency for Various Fan Maps with $\lambda/L = 1.65$

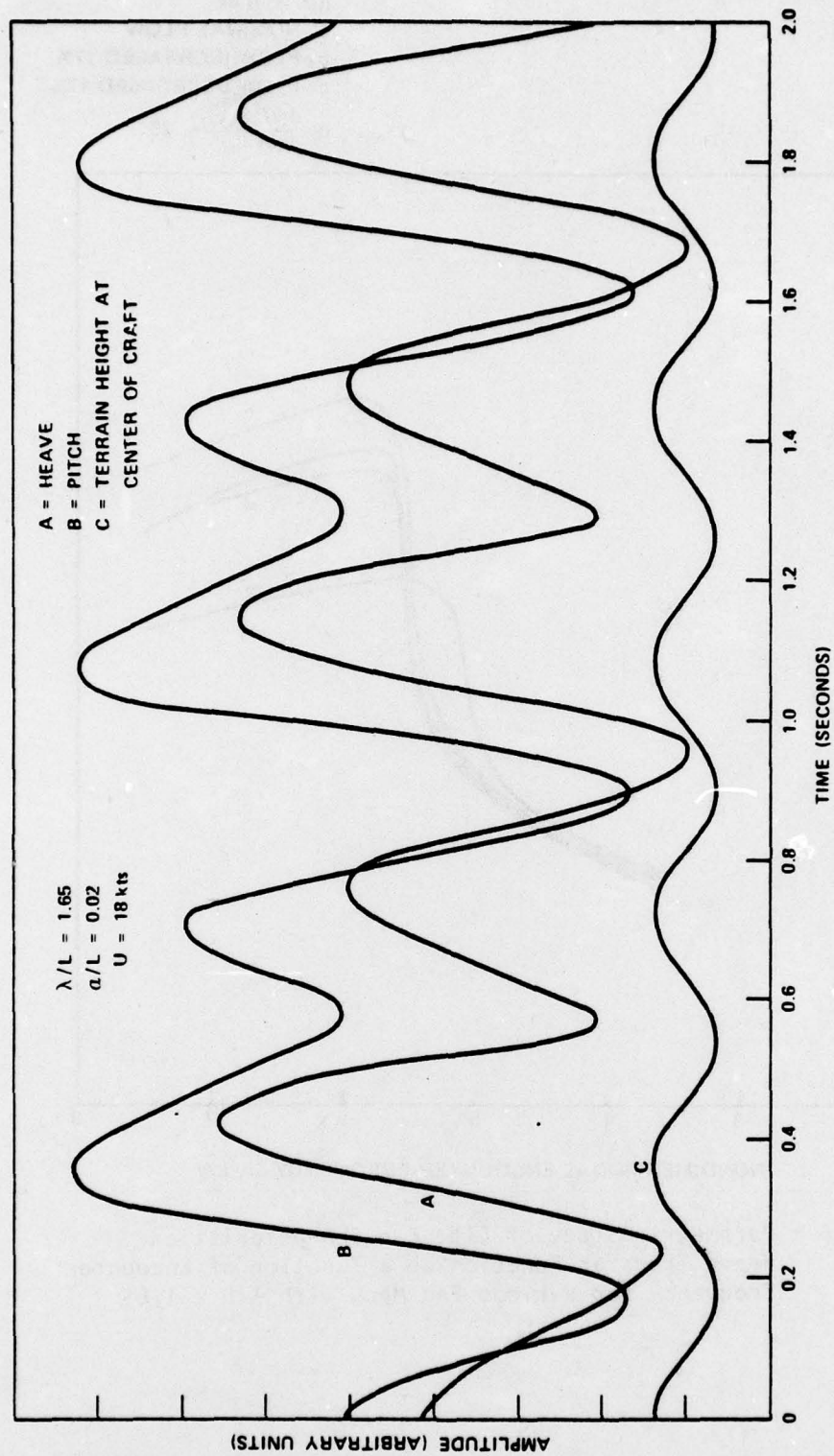


Figure 17 - Time-Dependent Pitch and Heave Simulation Responses for Sinusoidal Terrain at a Model Speed of 18 Knots

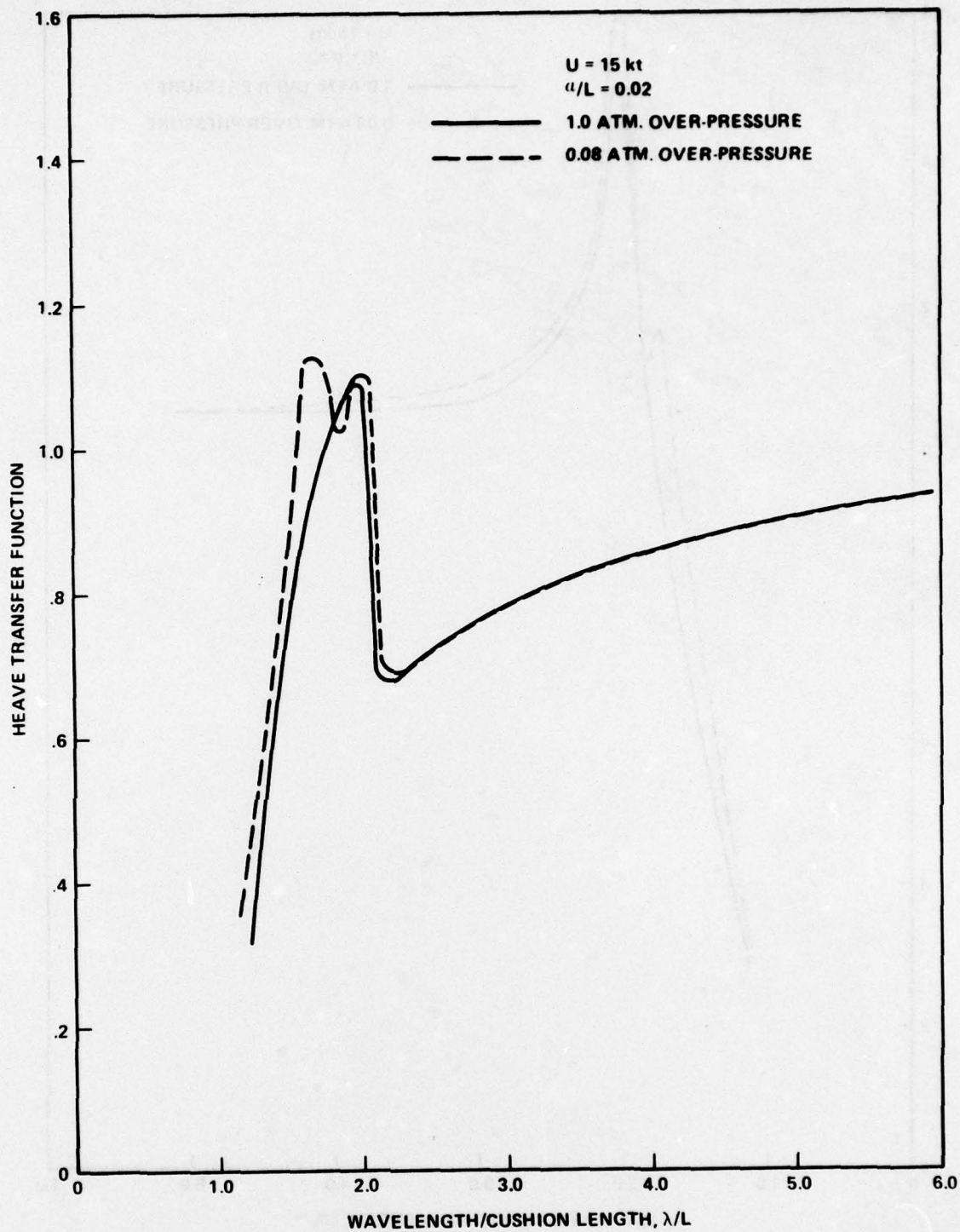


Figure 18 - Compressibility Effect on Model Scale Analytic Pitch Transfer Function as a Function of Wave Length for a Model Speed of 15 Knots

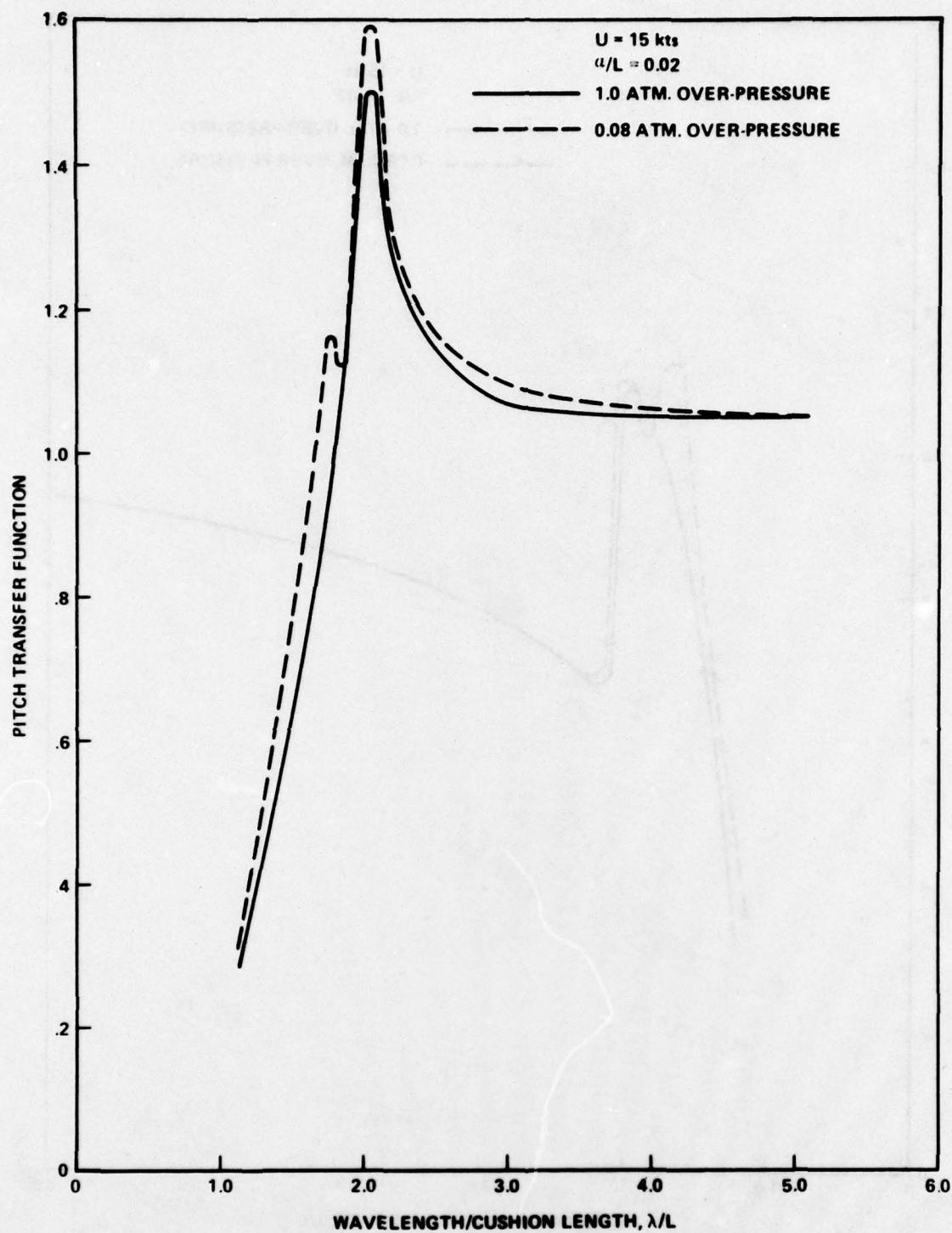


Figure 19 - Compressibility Effect on Model Scale Analytic Heave Transfer Function as a Function of Wave Length for a Model Speed of 15 Knots

DTNSRDC ISSUES THREE TYPES OF REPORTS

(1) DTNSRDC REPORTS, A FORMAL SERIES PUBLISHING INFORMATION OF PERMANENT TECHNICAL VALUE, DESIGNATED BY A SERIAL REPORT NUMBER.

(2) DEPARTMENTAL REPORTS, A SEMIFORMAL SERIES, RECORDING INFORMATION OF A PRELIMINARY OR TEMPORARY NATURE, OR OF LIMITED INTEREST OR SIGNIFICANCE, CARRYING A DEPARTMENTAL ALPHANUMERIC IDENTIFICATION.

(3) TECHNICAL MEMORANDA, AN INFORMAL SERIES, USUALLY INTERNAL WORKING PAPERS OR DIRECT REPORTS TO SPONSORS, NUMBERED AS TM SERIES REPORTS; NOT FOR GENERAL DISTRIBUTION.